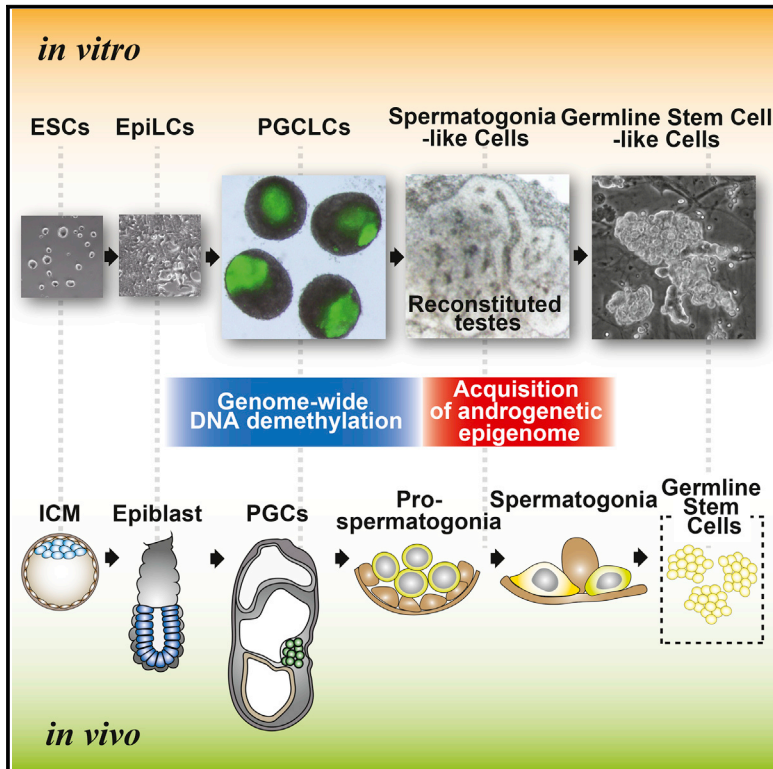# Cell Reports

In Vitro Derivation and Propagation of Spermatogonial Stem Cell Activity from Mouse Pluripotent Stem Cells

Graphical Abstract

Authors

Yukiko Ishikura, Yukihiro Yabuta, Hiroshi Ohta, ..., Kenjiro Shirane, Hiroyuki Sasaki, Mitinori Saitou

Correspondence

saitou@anat2.med.kyoto-u.ac.jp

In Brief

Ishikura et al. report the in vitro derivation and propagation of spermatogonial stem cells (SSCs) from mouse embryonic stem cells (ESCs). The authors show that appropriate regulation of genome-wide DNA methylation pattern is crucial for the in vitro derivation of SSCs with proper spermatogenic function.

Highlights

- In vitro derivation of mouse germline stem cell-like cells (GSCLCs) from ESCs

- GSCLCs colonize adult testes and contribute to spermatogenesis and fertile offspring

- GSCLCs show aberrant DNA methylation at vulnerable regulatory elements

- Spermatogonial stem cell induction relies on faithful regulation of DNA methylation

Accession Numbers

GSE76245
GSE87341

CrossMark

CellPress

In Vitro Derivation and Propagation of Spermatogonial Stem Cell Activity from Mouse Pluripotent Stem Cells

Yukiko Ishikura,[1,2] Yukihiro Yabuta,[1,2] Hiroshi Ohta,[1,2] Katsuhiko Hayashi,[1,3,4] Tomonori Nakamura,[1,2] Ikuhiro Okamoto,[1,2] Takuya Yamamoto,[5,6,7] Kazuki Kurimoto,[1,2] Kenjiro Shirane,[8,9] Hiroyuki Sasaki,[8,9] and Mitinori Saitou[1,2,5,6,10,*]

[1]Department of Anatomy and Cell Biology, Graduate School of Medicine, Kyoto University, Yoshida-Konoe-cho, Sakyo-ku, Kyoto 606-8501, Japan
[2]JST, ERATO, Yoshida-Konoe-cho, Sakyo-ku, Kyoto 606-8501, Japan
[3]JST, PRESTO, Maidashi 3-1-1, Higashi-ku, Fukuoka 812-8582, Japan
[4]Department of Developmental Stem Cell Biology, Faculty of Medical Sciences, Kyushu University, Maidashi 3-1-1, Higashi-ku, Fukuoka 812-8582, Japan
[5]Center for iPS Cell Research and Application, Kyoto University, 53 Kawahara-cho, Shogoin, Sakyo-ku, Kyoto 606-8507, Japan
[6]Institute for Integrated Cell-Material Sciences, Kyoto University, Yoshida-Ushinomiya-cho, Sakyo-ku, Kyoto 606-8501, Japan
[7]AMED-CREST, AMED, 1-7-1 Otemachi, Chiyoda-ku, Tokyo 100-0004, Japan
[8]Division of Epigenomics and Development, Medical Institute of Bioregulation, and Epigenome Network Research Center, Kyushu University, Maidashi 3-1-1, Higashi-ku, Fukuoka 812-8582, Japan
[9]Graduate School of Medical Sciences, Kyushu University, Maidashi 3-1-1, Higashi-ku, Fukuoka 812-8582, Japan
[10]Lead Contact
*Correspondence: saitou@anat2.med.kyoto-u.ac.jp
http://dx.doi.org/10.1016/j.celrep.2016.11.026

SUMMARY

The in vitro derivation and propagation of spermatogonial stem cells (SSCs) from pluripotent stem cells (PSCs) is a key goal in reproductive science. We show here that when aggregated with embryonic testicular somatic cells (reconstituted testes), primordial germ cell-like cells (PGCLCs) induced from mouse embryonic stem cells differentiate into spermatogonia-like cells in vitro and are expandable as cells that resemble germline stem cells (GSCs), a primary cell line with SSC activity. Remarkably, GSC-like cells (GSCLCs), but not PGCLCs, colonize adult testes and, albeit less effectively than GSCs, contribute to spermatogenesis and fertile offspring. Whole-genome analyses reveal that GSCLCs exhibit aberrant methylation at vulnerable regulatory elements, including those critical for spermatogenesis, which may restrain their spermatogenic potential. Our study establishes a strategy for the in vitro derivation of SSC activity from PSCs, which, we propose, relies on faithful epigenomic regulation.
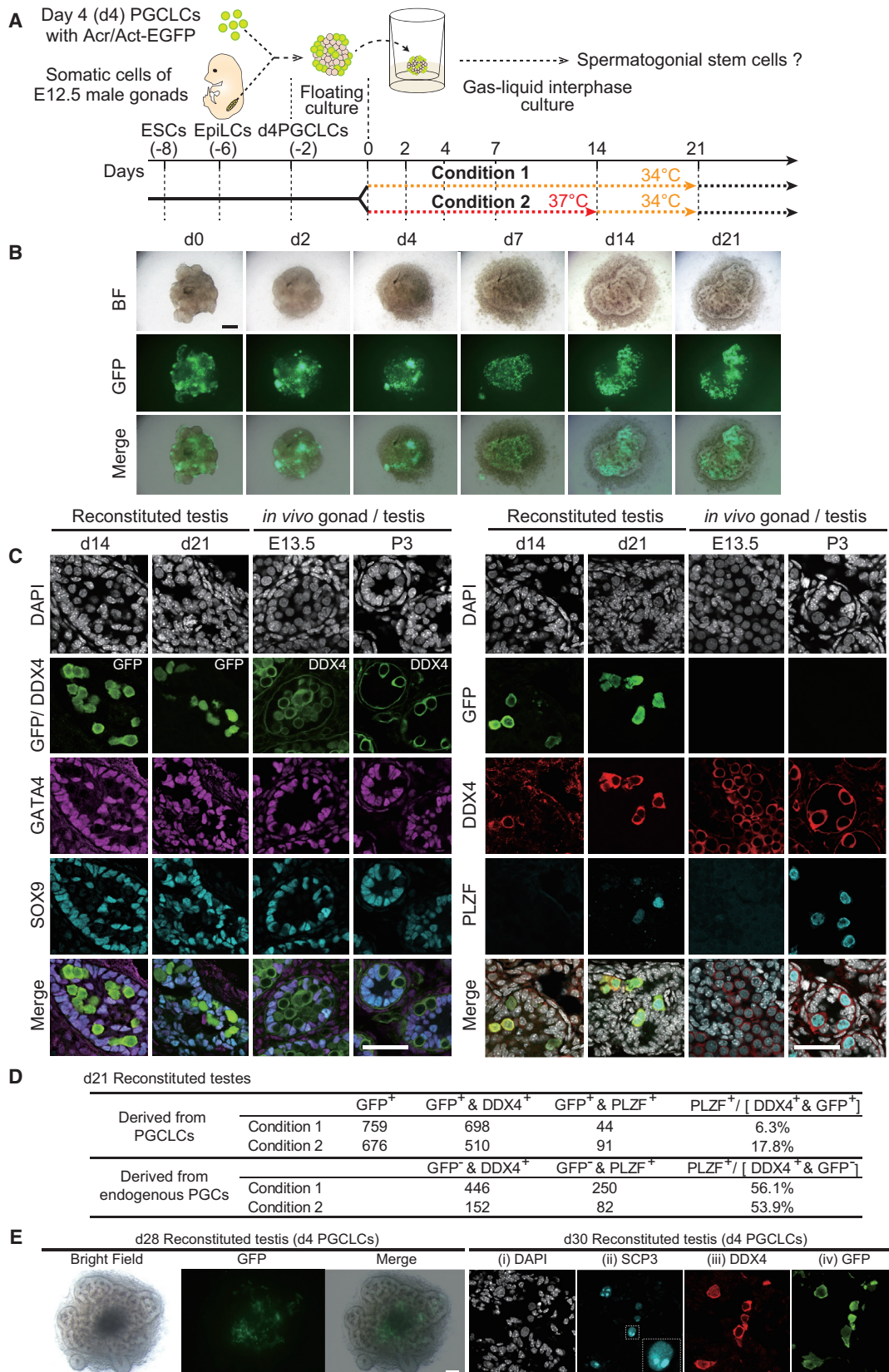
INTRODUCTION

Germ cells are a source of totipotency, underlying reproduction, inheritance, and evolution of a given species. In mice, the germ cell lineage is induced in the epiblast in response to signaling molecules at around embryonic day (E) 6.0 and is established in the extra-embryonic mesoderm as primordial germ cells (PGCs) by around E7.0 (Ginsburg et al., 1990; Lawson et al., 1999; Saitou et al., 2002). PGCs then initiate migration through the hindgut endoderm and colonize embryonic testes or ovaries at around E10.5, where they continue to proliferate until around E13.5 (Tam and Snow, 1981). A key event that takes place in PGCs is epigenomic reprogramming involving genome-wide DNA demethylation, which leads to erasure of parental imprints and X reactivation in females (Lee et al., 2014; Saitou et al., 2012).

In embryonic testes, PGCs enter mitotic arrest around E13.5 and differentiate into pro-spermatogonia in the luminal compartment of incipient seminiferous tubules (Hilscher et al., 1974) acquiring an androgenetic epigenome, including paternal imprints, by postnatal day (P) 5 (Kobayashi et al., 2013; Kubo et al., 2015; Seisenberger et al., 2012). Thereafter, pro-spermatogonia migrate into the basal compartment of the seminiferous tubules to differentiate as spermatogonia, which undergo first-wave spermatogenesis (Bellvé et al., 1977) or are recruited as spermatogonial stem cells (SSCs) that sustain spermatogenesis throughout the adult period (Kanatsu-Shinohara and Shinohara, 2013; Yang and Oatley, 2014). In contrast, in embryonic ovaries, from around E13.5, PGCs enter directly into the first prophase of the meiosis to differentiate into primary oocytes (Hilscher et al., 1974), which serve as a foundation for oogenesis (McGee and Hsueh, 2000).

Reconstitution of germ cell development in vitro will offer opportunities for understanding the mechanism of germ cell development both under normal and diseased conditions (Saitou and Miyauchi, 2016). It has been demonstrated that mouse pluripotent stem cells (PSCs) are induced into epiblast-like cells (EpiLCs), which are, in turn, induced into primordial germ cell-like cells (PGCLCs) with the capacity for both spermatogenesis and oogenesis: male PGCLCs contribute to spermatogenesis when transplanted into testes of neonatal mice lacking endogenous

A Day 4 (d4) PGCLCs with Acr/Act-EGFP

Somatic cells of E12.5 male gonads

Floating culture

Gas-liquid interphase culture

Spermatogonial stem cells ?

ESCs (-8) EpiLCs (-6) d4PGCLCs (-2) 0 2 4 7 14 21

Days

Condition 1 — 34°C

Condition 2 — 37°C — 34°C

B

d0   d2   d4   d7   d14   d21

BF

GFP

Merge

C

Reconstituted testis | *in vivo* gonad / testis

d14   d21   E13.5   P3

DAPI

GFP/ DDX4 — GFP GFP DDX4 DDX4

GATA4

SOX9

Merge

Reconstituted testis | *in vivo* gonad / testis

d14   d21   E13.5   P3

DAPI

GFP

DDX4

PLZF

Merge

D d21 Reconstituted testes

		GFP⁺	GFP⁺ & DDX4⁺	GFP⁺ & PLZF⁺	PLZF⁺/ [DDX4⁺ & GFP⁺]
Derived from PGCLCs	Condition 1	759	698	44	6.3%
	Condition 2	676	510	91	17.8%
			GFP⁻ & DDX4⁺	GFP⁻ & PLZF⁺	PLZF⁺/ [DDX4⁺ & GFP⁻]
Derived from endogenous PGCs	Condition 1		446	250	56.1%
	Condition 2		152	82	53.9%

E

d28 Reconstituted testis (d4 PGCLCs)

Bright Field   GFP   Merge

d30 Reconstituted testis (d4 PGCLCs)

(i) DAPI   (ii) SCP3   (iii) DDX4   (iv) GFP

(legend on next page)

spermatogenesis (*W/W^v* mice) (Hayashi et al., 2011), whereas female PGCLCs, when aggregated with somatic cells of female embryonic gonads and either transplanted under the ovarian bursa (Hayashi et al., 2012) or cultured appropriately (Hikabe et al., 2016), mature into fully grown oocytes. These spermatozoa and oocytes contribute to fertile offspring. A number of key issues associated with germ cell biology have been resolved based on this system (Saitou and Miyauchi, 2016). Moreover, human (h) PGCLCs have been induced from hPSCs (Irie et al., 2015; Sasaki et al., 2015), creating an opportunity for understanding the mechanism of human germ cell development in vitro.

A key next step for male germ cell development in vitro would be to induce PGCLCs into spermatogonia or SSC-like cells, the immediate precursors of spermatogenesis. Here, we set out to achieve such induction by exploiting "reconstituted testes" (Ohinata et al., 2009) in vitro.

RESULTS

PGCLCs Undergo Male Differentiation in Reconstituted Testes

Close interactions between germ cells and testicular somatic cells—particularly Sertoli cells—are essential for male germ cell differentiation (Svingen and Koopman, 2013). We sought to develop a culture system using reconstituted testes to explore whether PGCLCs undergo spermatogenic differentiation in vitro (Figure 1A). We induced embryonic stem cells (ESCs) bearing *Acro/Act-EGFP* (AAG) transgenes (129/SvJcl × C57BL/6 background) (Ohta et al., 2000) into PGCLCs, isolated them at day (d) 4 or d6 PGCLCs based on high levels of SSEA1 and INTEGRINβ3 using fluorescence-activated cell sorting (FACS), and generated aggregates of PGCLCs with embryonic testicular cells at embryonic day (E) 12.5 depleted of PGCs by magnetic cell sorting (MACS) (Figure 1A). After culturing for 2 days under floating conditions, we placed the reconstituted testes on a permeable membrane for a gas-liquid interphase culture (Steinberger et al., 1964) either at 34°C (condition 1) or at 37°C for 2 weeks followed by 34°C for the remaining period (condition 2) (Figure 1A). Since d6 PGCLCs did not integrate well with reconstituted testes for unknown reasons (data not shown), we used d4 PGCLCs as starting materials. Since we obtained similar results under both conditions 1 and 2, we present representative results from either condition.

At d0 of the gas-liquid interphase culture, the reconstituted testes exhibited a flat and round shape with no obvious substructures (Figures 1B and S1A). AAG-positive (+) cells showed

a random distribution throughout reconstituted testes with the formation of several clumps (Figures 1B and S1A). From around d4, seminiferous tubule-like structures began to be evident, and at d7, they exhibited extensive development and assembled an anastomosed network (Figures 1B and S1A). By d7, AAG (+) cells, including clumps, outside the seminiferous tubule-like structures disappeared, and the vast majority of the AAG (+) cells were inside the seminiferous tubule-like network (Figures 1B and S1A). Thereafter, the reconstituted testes were maintained stably with further development of the seminiferous tubule-like network, and the AAG (+) cells within the network appearing to increase in number (Figures 1B and S1A).

Immunofluorescence (IF) analysis of the reconstituted testes at d14 and d21 revealed robust seminiferous tubule-like structures delineated by cells positive for GATA4 and SOX9, key transcription factors for Sertoli cells (Vidal et al., 2001; Viger et al., 1998), which were underlain by a layer of squamous cells, most likely myoid cells (Figures 1C and S1B). The AAG (+) cells with characteristic nuclear architecture were present almost exclusively within the luminal compartment of seminiferous tubules at d14 and many of them were found in the basal compartment at d21 (Figures 1C and S1B). At d14, many of the AAG (+) cells became (+) for DDX4, a germ cell marker that begins expression in gonadal PGCs (Fujiwara et al., 1994), but were negative for PLZF (ZBTB16), an SSC marker that initiates expression perinatally in pro-spermatogonia (Buaas et al., 2004; Costoya et al., 2004) (Figures 1C and S1B). At d21, some of the AAG (+) cells became both DDX4 and PLZF (+) (Figures 1C and S1B). We examined sections throughout a reconstituted testis at d21 under each condition: a majority of AAG (+) cells became DDX4 (+) (~92% for condition 1 and ~75% for condition 2) and a fraction of DDX4 (+) cells became PLZF (+) (~6.3% for condition 1 and ~18% for condition 2) (Figure 1D). Interestingly, we noted that endogenous PGCs that remained to be depleted by MACS (AAG (−)/DDX4 (+)) acquired PLZF at a higher frequency than d4 PGCLCs (~56% for condition 1 and ~54% for condition 2) (Figures 1D and S1C).

We performed longer cultures of reconstituted testes (until d54): although a few AAG (+) cells or endogenous germ cells were positive for SCP3, a key marker for the onset of meiosis (Figures 1E and S1D) (Yuan et al., 2000), we did not find cells that completed meiosis under our conditions. Collectively, these data indicate that the reconstituted testes in vitro recapitulate testis development, and, within the reconstituted testes, PGCLCs undergo differentiation to form spermatogonia-like cells. The kinetics of differentiation of PGCLCs into such cell types was protracted compared to that of PGCs in vivo.

Figure 1. Development of Reconstituted Testes In Vitro

(A) Scheme for the generation and culture of reconstituted testes under two conditions.

(B) Representative images of the development of reconstituted testes over 3 weeks (condition 2). Bright-field images (BF), AAG fluorescence, and their merges are shown. Bar, 200 μm.

(C) GATA4 and SOX9 (left) or DDX4 and PLZF (right) expression in reconstituted testes at d14 and d21 (condition 2) or in testes at E13.5 and P3. Bars, 50 μm. PGCLC-derived cells and endogenous germ cells are identified by GFP and DDX4, respectively (second rows). DAPI staining and merges are also shown.

(D) Rates of differentiation of d4 PGCLCs or E12.5 PGCs into DDX4 (+)/PLZF (−) and DDX4 (+)/PLZF (+) cells in reconstituted testes.

(E) Prolonged cultures of reconstituted testes (condition 1). (left) Morphology of a reconstituted testis cultured for 28 days. Bar, 200 μm. (right) DDX4 (ii), SCP3 (iii), and GFP (iv) expression of a section of a reconstituted testis cultured for 30 days. (i) DAPI. Bar, 10 μm.

See also Figure S1.
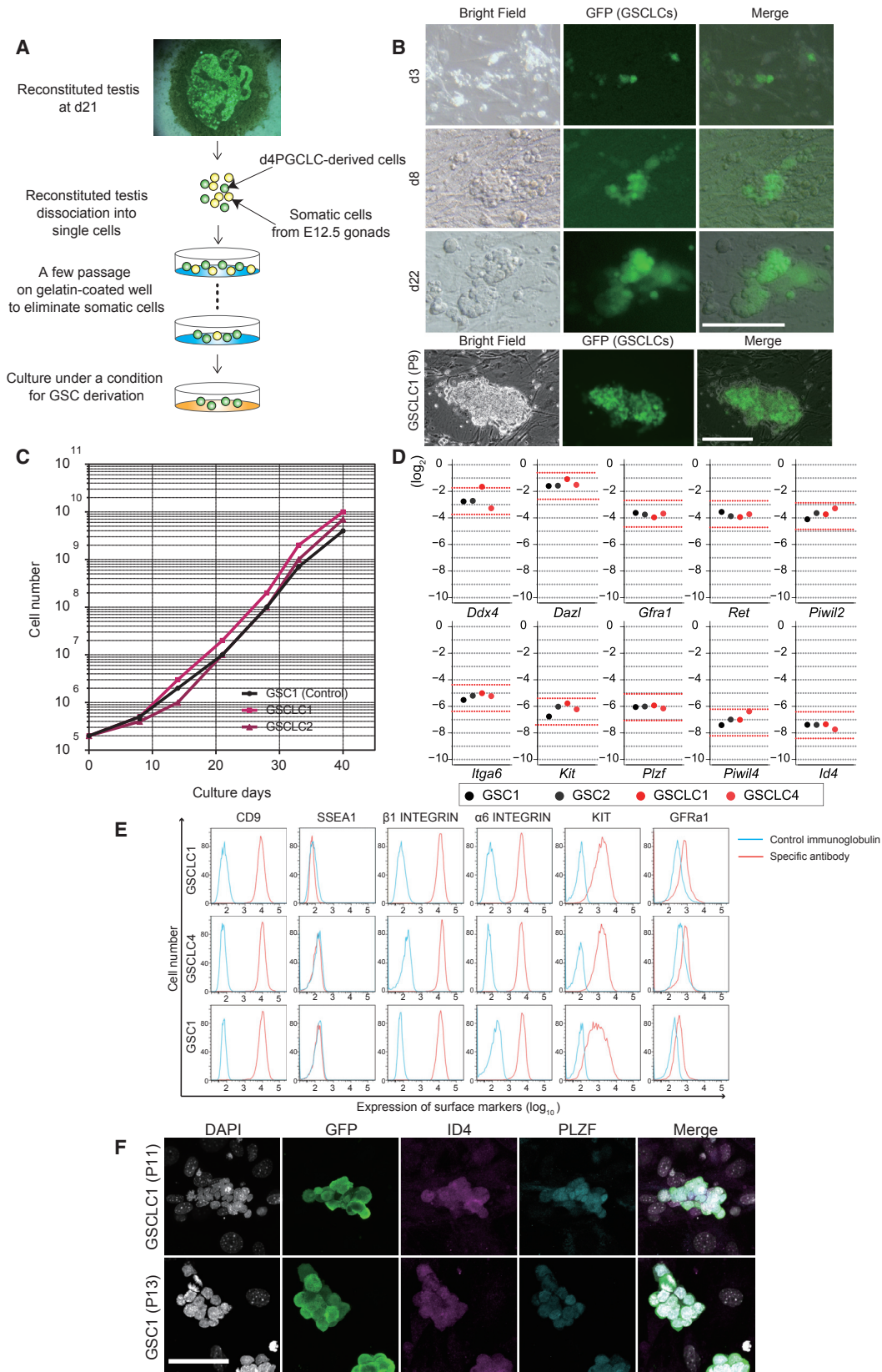
(legend on next page)

Propagation In Vitro of a Spermatogonia-like State from PGCLCs

Perinatal pro-spermatogonia, spermatogonia, or SSCs, but not PGCs, can be propagated in vitro as a primary cell line with the capacity for self-renewal and spermatogenesis, referred to as germline stem cells (GSCs) (Kanatsu-Shinohara et al., 2003; Kubota et al., 2004). Neonatal testes are a robust source for derivation of GSCs (Kanatsu-Shinohara et al., 2003). We therefore examined whether we can derive GSC-like cells (GSCLCs) from d21 reconstituted testes, which bear PGCLC-derived spermatogonia-like cells and may resemble neonatal testes. The d21 reconstituted testes were dissociated into single cells, and the AAG (+) cells were enriched and cultured under GSC derivation conditions (Figure 2A). At d3 of culture, AAG (+) cells were scattered on mouse embryonic feeders (MEFs) as single or pairs of cells (a few thousand cells from a single reconstituted testis), a few of which, at d8, formed small colonies (at most a few dozen colonies) (Figure 2B). Thereafter, such colonies exhibited slow proliferation and, upon several passages, were propagated as stable cell lines bearing a grape cluster-like colony morphology indistinguishable from that of GSCs, with normal karyotype (nine and six lines from conditions 1 and 2, respectively), and with high efficiency for cryopreservation/re-expansion followed by thawing (Figures 2B and S2A). We were able to establish such lines in a consistent fashion when the initial colony numbers were more than ten, and they were propagated similarly to GSCs (129/SvJcl × C57BL/6) (Figure 2C) (Kanatsu-Shinohara et al., 2003).

We compared the expression of key genes (*Ddx4*, *Dazl*, *Gfra1*, *Ret*, *Piwil2*, *Itga6*, *Kit*, *Plzf*, *Piwil4*, and *Id4*), surface markers (CD9, SSEA1, INTEGRINβ1, INTEGRINα6, KIT, and GFRα1), and transcription factors (PLZF and ID4) (Kanatsu-Shinohara and Shinohara, 2013; Yang and Oatley, 2014) in reconstituted testis-derived cell lines with those in GSCs, which revealed that they exhibit similar gene expression to GSCs (Figures 2D–2F). We thus refer to these cell lines as GSCLCs. To examine whether GSCLCs can be derived from PGCLCs without the formation of reconstituted testes, we cultured d4 or d6 PGCLCs sorted by SSEA1 and INTEGRINβ3 directly under the GSC-derivation conditions. This, however, resulted in a rapid expansion (within a few days) of strongly alkaline phosphatase-positive, dome-shaped ESC-like colonies with efficiencies similar to those of embryonic germ cell (EGC) derivation from PGCs (~5%) (Figure S2B) (Matsui et al., 1992; Resnick et al., 1992), and we were unable to isolate/detect GSC-like colonies from such cultures.

We conclude that the differentiation of PGCLCs into the male germ cell pathway is essential for the derivation of GSCLCs.

Spermatogenesis in Adult Testes and Fertile Offspring from GSCLCs

Spermatogonia/SSCs can colonize adult testes (approximately >8 weeks) for spermatogenesis (Brinster and Zimmermann, 1994), whereas PGCs colonize and undergo spermatogenesis only in neonatal testes (~5–10 days) (Chuma et al., 2005; Ohta et al., 2004). This would be due to the difference either of homing capacity or of intrinsic/epigenetic capacities for spermatogenesis between these cell types.
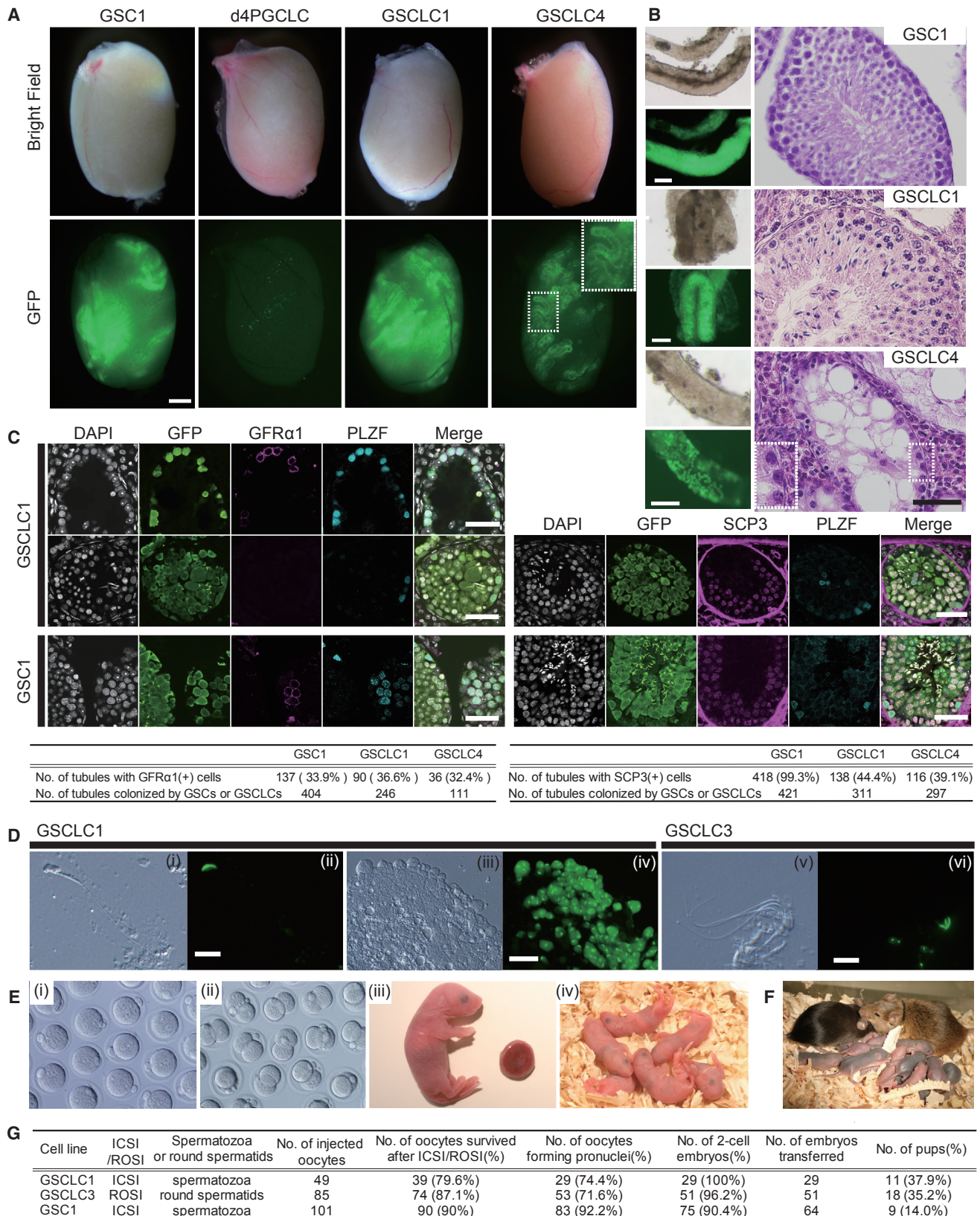
To examine whether GSCLCs acquire a mature stem cell property, we transplanted them into adult testes (8–10 weeks) of *W/Wv* mice. GSCs (AAG (+); 129/SvJcl × C57BL/6) (GSC1) robustly colonized adult testes and underwent spermatogenesis (Figure 3A), whereas PGCLCs failed to show such activity in adults (Figure 3A), although they did so in neonates (Hayashi et al., 2011). Remarkably, unlike PGCLCs, all the GSCLC lines colonized the adult testes (Figures 3A, S3A, and S3B). However, somewhat unexpectedly, a few of them (GSCLC1, 2, 3: 3/15) underwent spermatogenesis in a fraction of colonized tubules (Figures 3A, S3A, and S3B). Histological analyses confirmed that proper spermatogenesis occurred in the tubules fully occupied by GSCLC-derived AAG (+) cells (Figure 3B), whereas only spermatogonia or cells at the first meiotic prophase were present in the tubules bearing aligned chains of AAG (+) cells only around the basal compartment (Figure 3B). No GSCLC lines formed teratomas in transplanted testes, at least until 16 weeks after transplantation.

IF analyses revealed that GFRα1 (+) spermatogonia/SSC-like cells were present at a similar ratio in tubules colonized by GSCs (~33.9%) and GSCLCs (GSCLC1: ~36.6%; 4: ~32.4%) (Figure 3C). In contrast, while nearly all the tubules colonized by GSCs exhibited SCP3 (+) meiocytes (~99.3%), less than half of the tubules colonized by GSCLCs (GSCLC1: ~44.4%; 4: ~39.1%) showed such cells (Figure 3C). Thus, GSCLCs colonize adult seminiferous tubules and exhibit characteristics of spermatogonia/SSCs: however, they have a tendency to halt spermatogenesis at around the entry into or early stages of the first meiotic prophase.

We examined the function of GSCLC-derived spermatozoa or spermatids. We were able to isolate such cells (GSCLC1: spermatozoa; 3: round spermatids) consistently from seminiferous tubules with successful spermatogenesis (Figure 3D) and

---

Figure 2. Derivation of Germline Stem Cell-like Cells from Reconstituted Testes

(A) Scheme for GSCLC derivation from reconstituted testes.

(B) (top) Representative images for colonies of AAG (+) cells during the derivation of GSCLCs. BF images, AAG fluorescence, and their merges are shown. (bottom) Images for a GSCLC line (GSCLC1) at passage 9. Bars, 100 μm.

(C) Growth of GSCLCs (GSCLC1, 2) and GSCs (GSC1). 2 × 10^5 GSCLCs/GSCs were plated, and their proliferation was evaluated every 6 or 7 days.

(D) Expression levels of the indicated genes as measured by qPCR in GSCLCs (GSCLC1, 4) and GSCs (GSC1, 2). For each gene, the ⊿Ct (the threshold-cycle [Ct] value difference) from the average Ct values of the two housekeeping genes *Arbp* and *Ppia* (set as 0) was plotted. The red dotted lines indicate the Ct values ±1 of the average Cts of GSCs.

(E) Expression levels (red plots) of the indicated surface markers as measured by FACS analyses in GSCLCs (GSCLC1, 4) and GSCs (GSC1). Blue plots indicate the fluorescence intensities by isotype-matched control antibodies.

(F) GFP, ID4, and PLZF expression with DAPI and their merges in a colony of GSCLCs (GSCLC1) and GSCs (GSC1). Bar, 50 μm.

See also Figure S2.

A

GSC1 | d4PGCLC | GSCLC1 | GSCLC4

Bright Field

GFP

B

GSC1

GSCLC1

GSCLC4

C

DAPI | GFP | GFRα1 | PLZF | Merge

GSCLC1

GSC1

	GSC1	GSCLC1	GSCLC4
No. of tubules with GFRα1(+) cells	137 (33.9%)	90 (36.6%)	36 (32.4%)
No. of tubules colonized by GSCs or GSCLCs	404	246	111

DAPI | GFP | SCP3 | PLZF | Merge

	GSC1	GSCLC1	GSCLC4
No. of tubules with SCP3(+) cells	418 (99.3%)	138 (44.4%)	116 (39.1%)
No. of tubules colonized by GSCs or GSCLCs	421	311	297

D GSCLC1 | GSCLC3

(i) (ii) (iii) (iv) (v) (vi)

E (i) (ii) (iii) (iv) **F**

G

Cell line	ICSI /ROSI	Spermatozoa or round spermatids	No. of injected oocytes	No. of oocytes survived after ICSI/ROSI(%)	No. of oocytes forming pronuclei(%)	No. of 2-cell embryos(%)	No. of embryos transferred	No. of pups(%)
GSCLC1	ICSI	spermatozoa	49	39 (79.6%)	29 (74.4%)	29 (100%)	29	11 (37.9%)
GSCLC3	ROSI	round spermatids	85	74 (87.1%)	53 (71.6%)	51 (96.2%)	51	18 (35.2%)
GSC1	ICSI	spermatozoa	101	90 (90%)	83 (92.2%)	75 (90.4%)	64	9 (14.0%)

(legend on next page)

performed intra-cytoplasmic sperm injection (ICSI) or round spermatid injection (ROSI), respectively, which resulted in the generation of apparently normal offspring in normal ratios (Figures 3E and 3G). Such offspring bore proper imprints as examined by combined bisulfite restriction analysis (COBRA), exhibited grossly normal development, and were fertile (Figures 3F and S3C–S3E). Thus, through PGCLCs and their differentiation into the male pathway in reconstituted testes, PSCs can be induced into a stable cell line with SSC capacity, an immediate precursor for spermatogenesis in adult testes.

Transcription and DNA Methylation Analysis of GSCLCs

The development of spermatogonia/SSCs from PGCs involves genome-wide DNA demethylation followed by acquisition of an androgenic methylome (Kobayashi et al., 2013; Kubo et al., 2015; Seisenberger et al., 2012). The limited spermatogenic capacity of GSCLCs derived under the present conditions might have resulted from impaired transcription/transcriptional potential associated with epigenetic mis-regulation during their derivation.

Transcriptome

We compared the transcriptomes of GSCLCs (GSCLC1-4) with those of GSCs (GSC1, 2) using RNA sequencing (RNA-seq) (Figures S4A and S4B) (Nakamura et al., 2015). Consistent with the analyses of the expression of key markers (Figures 2D–2F), unsupervised hierarchical clustering (UHC) and principal component analysis (PCA) clustered GSCLCs and GSCs together in comparison to ESCs, EpiLCs, and d4/d6 PGCLCs (Figures 4A and 4B), demonstrating that GSCLCs acquire a transcriptome similar to that of GSCs.

The GSCLCs and GSCs, however, were segregated upon mutual comparison, and each GSCLC line formed a separate cluster (Figure 4C). We identified differentially expressed genes (DEGs) between each GSCLC line and the averages of two GSC lines (Figures 4D, 4E, S4C, and S4D). The DEGs accounted for ~2.5% to ~4.5% of the genes expressed among GSCs/GSCLCs (Figure 4D), and GSCLC1 with better spermatogenic activity (Figures 3 and S3) exhibited the smallest number of DEGs, whereas GSCLC4 with no spermatogenic activity (Figures 3 and S3) showed the largest number of DEGs (Figure 4D). Genes downregulated in GSCLCs (407 in total) were higher in number than those upregulated (355 in total) and DEGs in each GSCLC line partially overlapped (Figures 4D and S4C). The genes commonly downregulated in all four GSCLC lines (55 genes)

included a key pluripotency gene (Pou5f1) (Ohbo et al., 2003), genes implicated in the self-renewal of SSCs (Lhx1, T) (Oatley et al., 2006; Wu et al., 2011), and those critical for meiosis/repression of transposons through DNA methylation (Tex19.1, Tdrd9) (Ollinger et al., 2008; Shoji et al., 2009). Both the intersection and union of genes downregulated in GSCLCs were enriched with gene ontology (GO) functional terms such as "anterior/posterior pattern formation" (Hoxb2, Hoxb3, Hoxb5-9, Lhx1, T, Wnt3, and Sfrp2, etc.) (Figures 4D and 4E; Table S1).

Global DNA Methylation Profiles

We next analyzed the genome-wide DNA methylation profiles of GSCLCs (GSCLC1-4) in comparison to those of GSCs (GSC1, 2) and d4 PGCLCs by whole-genome bisulfite sequencing (WGBS). Although bisulfite sequencing does not discriminate between 5-methylcytosine (5mC) and 5-hydroxymethylcytosine (5hmC) (Hayatsu and Shiragami, 1979), since 5hmC consists only of a fraction of 5mC in germ cells (Shirane et al., 2016), we collectively designate 5mC and 5hmC as 5mC. We also examined the 5mC profiles of other key cell types reported previously (E10.5 PGCs, E13.5 PGCs, E16.5 pro-spermatogonia, P0 pro-spermatogonia, P7 KIT (−) spermatogonia, P7 KIT (+) spermatogonia, sperm, and MEFs [largely C57BL/6 background]) (Kobayashi et al., 2013; Kubo et al., 2015). We analyzed the 5mC levels in all CpG sites, across the genome-wide single-copy loci (2-Kb non-overlapping windows), in promoters (sequences 0.9 Kb upstream and 0.4 Kb downstream of the transcription start sites [TSSs] for 22,837 genes, which were classified into high [11,932], intermediate [3,381], and low [7,524] CpG density promoters [HCPs, ICPs, and LCPs, respectively] [Weber et al., 2007]), and in non-promoter CpG islands (CGIs: exons [2,574], introns [1,399], and intergenic regions [6,815]) (Illingworth et al., 2010) (Figures S5A and S5B).

Genome-wide 5mC levels were similar between GSCLCs (average: ~81.7%) and GSCs (~80.7%) (Figure S5B; Table S2). Figure 5A represents the 5mC-level tracks across chromosome 1 of the cell types analyzed: as reported previously (Kobayashi et al., 2013; Kubo et al., 2015), PGCs at E10.5 and, in particular, at E13.5, are depleted of the vast majority of 5mC and exhibit an extremely low 5mC level. Pro-spermatogonia at E16.5 gain a significant level of 5mC, except around the lamina-associated domains (LADs) (Guelen et al., 2008), and pro-spermatogonia at postnatal day (P) 0 show a nearly fully methylated pattern similar to spermatogonia at P7 that are (−) or (+) for KIT and mature spermatozoa (Figure 5A).

Figure 3. Spermatogenesis and Fertile Offspring from GSCLCs

(A and B) Representative BF and AAG-fluorescence images of testes (A) or isolated seminiferous tubules (B) of W/W^v mice 10 weeks after transplantation of GSCs (GSC1), d4 PGCLCs (only in A), and GSCLCs (GSCLC1, 4). The boxed area is magnified, revealing that AAG (+) cells were colonized only at the basal area of seminiferous tubules. The dotted fluorescence seen in the d4 PGCLC transplant (second left, bottom) is autofluorescence. Histological sections stained by H&E are shown in (B). Bar in (A), 1 mm; bars in (B), 100 μm (left) 50 μm (right).

(C) (top) GFP, GFRα1, and PLZF (left) or GFP, SCP, and PLZF (right) expression with DAPI and their merges in sections of seminiferous tubules of W/W^v mice 10 weeks after transplantation of GSCLCs (GSCLC1) or GSCs (GSC1). Bar, 50 μm. (bottom) Representative rates of seminiferous tubules with GFRα1 (+) (left) or SCP3 (+) (right) cells among tubules colonized by transplanted GSCs (GSC1) or GSCLCs (GSCLC1, 4).
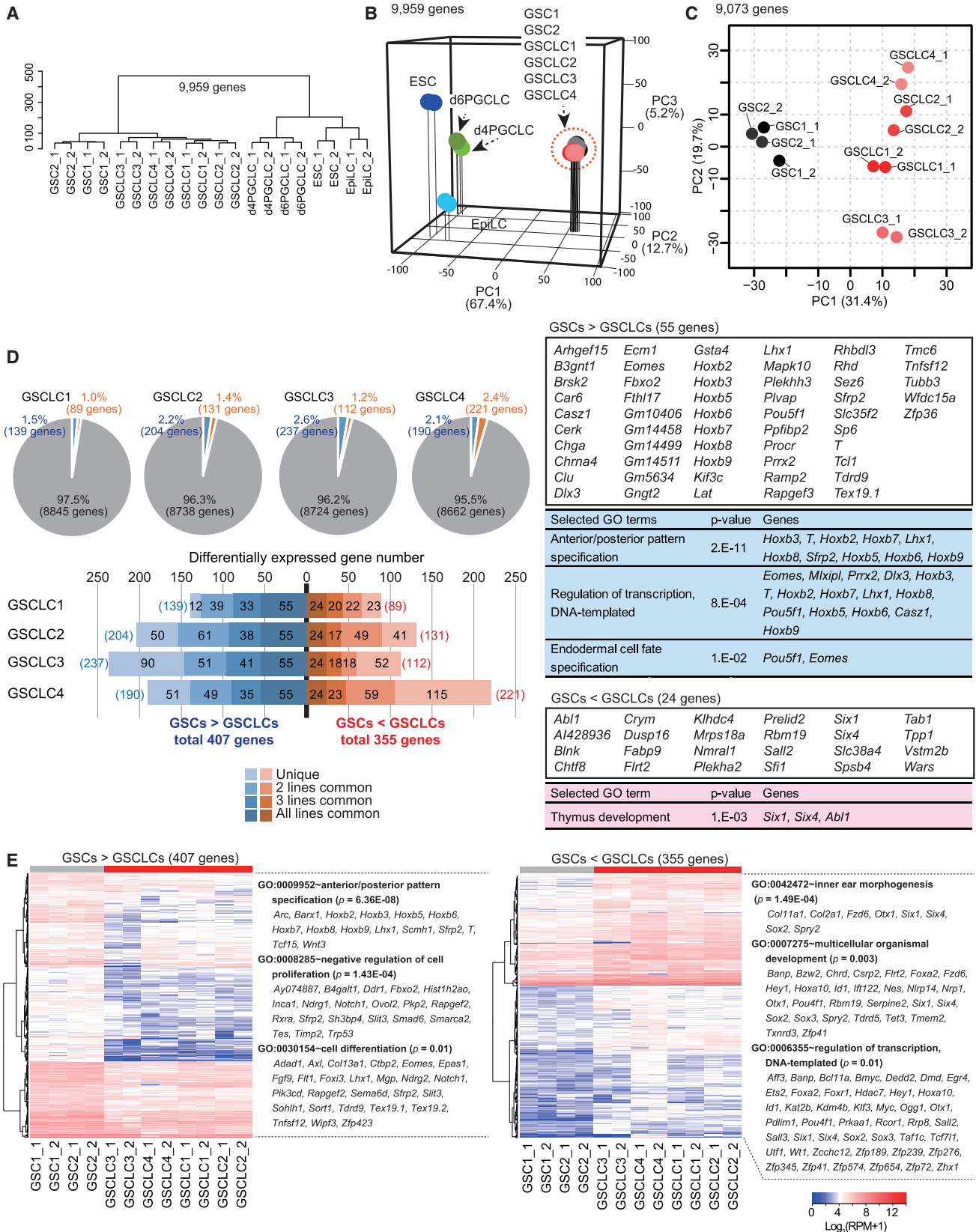
(D) BF (i, iii, v) and AAG-fluorescence (ii, iv, vi) images of spermatozoa (I, ii, v, vi) and spermatids (iii, iv) derived from GSCLC1 (i-iv) or GSCLC3 (v, vi). Bars in (ii, vi), 10 μm. Bar in (iv), 50 μm.

(E) Zygotes at pronuclear stages (i), 2-cell embryos (ii), offspring (iii, iv), and placenta (iii) produced by ICSI of GSCLC-derived spermatozoa.

(F) A fertile male offspring (agouti) from a GSCLC1-derived spermatozoon.

(G) Development of oocytes injected with spermatozoa derived from GSCLCs and GSCs.

See also Figure S3.

A 9,959 genes

B 9,959 genes

C 9,073 genes

D

GSCLC1 1.0% (89 genes) 1.5% (139 genes) 97.5% (8845 genes)

GSCLC2 1.4% (131 genes) 2.2% (204 genes) 96.3% (8738 genes)

GSCLC3 1.2% (112 genes) 2.6% (237 genes) 96.2% (8724 genes)

GSCLC4 2.4% (221 genes) 2.1% (190 genes) 95.5% (8662 genes)

Differentially expressed gene number

	250 200 150 100 50	0	50 100 150 200 250
GSCLC1	(139) 12 39 33 55		24 20 22 23 (89)
GSCLC2	(204) 50 61 38 55		24 17 49 41 (131)
GSCLC3	(237) 90 51 41 55		24 18 18 52 (112)
GSCLC4	(190) 51 49 35 55		24 23 59 115 (221)

GSCs > GSCLCs total 407 genes

GSCs < GSCLCs total 355 genes

Unique
2 lines common
3 lines common
All lines common

GSCs > GSCLCs (55 genes)

Arhgef15	Ecm1	Gsta4	Lhx1	Rhbdl3	Tmc6
B3gnt1	Eomes	Hoxb2	Mapk10	Rhd	Tnfsf12
Brsk2	Fbxo2	Hoxb3	Plekhh3	Sez6	Tubb3
Car6	Fthl17	Hoxb5	Plvap	Sfrp2	Wfdc15a
Casz1	Gm10406	Hoxb6	Pou5f1	Slc35f2	Zfp36
Cerk	Gm14458	Hoxb7	Ppfibp2	Sp6	
Chga	Gm14499	Hoxb8	Procr	T	
Chrna4	Gm14511	Hoxb9	Prrx2	Tcl1	
Clu	Gm5634	Kif3c	Ramp2	Tdrd9	
Dlx3	Gngt2	Lat	Rapgef3	Tex19.1	

Selected GO terms	p-value	Genes
Anterior/posterior pattern specification	2.E-11	Hoxb3, T, Hoxb2, Hoxb7, Lhx1, Hoxb8, Sfrp2, Hoxb5, Hoxb6, Hoxb9
Regulation of transcription, DNA-templated	8.E-04	Eomes, Mlxipl, Prrx2, Dlx3, Hoxb3, T, Hoxb2, Hoxb7, Lhx1, Hoxb8, Pou5f1, Hoxb5, Hoxb6, Casz1, Hoxb9
Endodermal cell fate specification	1.E-02	Pou5f1, Eomes

GSCs < GSCLCs (24 genes)

Abl1	Crym	Klhdc4	Prelid2	Six1	Tab1
AI428936	Dusp16	Mrps18a	Rbm19	Six4	Tpp1
Blnk	Fabp9	Nmral1	Sall2	Slc38a4	Vstm2b
Chtf8	Flrt2	Plekha2	Sfi1	Spsb4	Wars

Selected GO term	p-value	Genes
Thymus development	1.E-03	Six1, Six4, Abl1

E

GSCs > GSCLCs (407 genes)

GO:0009952~anterior/posterior pattern specification (p = 6.36E-08)
Arc, Barx1, Hoxb2, Hoxb3, Hoxb5, Hoxb6, Hoxb7, Hoxb8, Hoxb9, Lhx1, Scmh1, Sfrp2, T, Tcf15, Wnt3

GO:0008285~negative regulation of cell proliferation (p = 1.43E-04)
Ay074887, B4galt1, Ddr1, Fbxo2, Hist1h2ao, Inca1, Ndrg1, Notch1, Ovol2, Pkp2, Rapgef2, Rxra, Sfrp2, Sh3bp4, Slit3, Smad6, Smarca2, Tes, Timp2, Trp53

GO:0030154~cell differentiation (p = 0.01)
Adad1, Axl, Col13a1, Ctbp2, Eomes, Epas1, Fgf9, Flt1, Foxi3, Lhx1, Mgp, Ndrg2, Notch1, Pik3cd, Rapgef2, Sema6d, Sfrp2, Slit3, Sohlh1, Sort1, Tdrd9, Tex19.1, Tex19.2, Tnfsf12, Wipf3, Zfp423

GSCs < GSCLCs (355 genes)

GO:0042472~inner ear morphogenesis (p = 1.49E-04)
Col11a1, Col2a1, Fzd6, Otx1, Six1, Six4, Sox2, Spry2

GO:0007275~multicellular organismal development (p = 0.003)
Banp, Bzw2, Chrd, Csrp2, Flrt2, Foxa2, Fzd6, Hey1, Hoxa10, Id1, Ift122, Nes, Nlrp14, Nrp1, Otx1, Pou4f1, Rbm19, Serpine2, Six1, Six4, Sox2, Sox3, Spry2, Tdrd5, Tet3, Tmem2, Txnrd3, Zfp41

GO:0006355~regulation of transcription, DNA-templated (p = 0.01)
Aff3, Banp, Bcl11a, Bmyc, Dedd2, Dmd, Egr4, Ets2, Foxa2, Foxr1, Hdac7, Hey1, Hoxa10, Id1, Kat2b, Kdm4b, Klf3, Myc, Ogg1, Otx1, Pdlim1, Pou4f1, Prkaa1, Rcor1, Rrp8, Sall2, Sall3, Six1, Six4, Sox2, Sox3, Taf1c, Tcf7l1, Utf1, Wt1, Zcchc12, Zfp189, Zfp239, Zfp276, Zfp345, Zfp41, Zfp574, Zfp654, Zfp72, Zhx1

0 4 8 12
Log₂(RPM+1)

(legend on next page)

d4 PGCLCs showed an average 5mC level of ~50.5%, which is higher than that of E10.5 and E13.5 PGCs (average: ~16.2% and ~3.8%, respectively) (Figures 5A and S5B) (Kobayashi et al., 2013; Shirane et al., 2016). Notably the overall configuration of the methylome of d4 PGCLCs is similar to that of E10.5 PGCs, with relatively flat 5mC levels across the chromosome (Figure 5A), indicating that d4 PGCLCs bear a methylome corresponding to earlier PGCs, and such a configuration would represent the methylome in the middle of genome-wide DNA demethylation (Shirane et al., 2016). In contrast, both GSCLCs and GSCs showed methylation profiles similar to those of postnatal spermatogenic cells with common low methylated regions (LMRs) (Stadler et al., 2011) (Figure 5A). Thus, at a global level, compared to PGCLCs/PGCs, GSCLCs and GSCs bear similar DNA methylomes both to each other and to postnatal spermatogenic cells.

DNA Methylation at Regulatory Elements

On the other hand, GSCLCs showed 5mC levels consistently higher than GSCs in promoters and non-promoter CGIs (Figure S5B). Accordingly, PCA of the 5mC profiles of promoters and non-promoter CGIs clustered GSCLCs apart from GSCs and postnatal spermatogenic cells (Figure S5C). Scatterplot comparisons revealed that, while GSCs and KIT (−) spermatogonia at P7 showed similar 5mC-level distributions across such regions (Figure S5D), GSCLCs bear promoters (particularly LCPs) and non-promoter CGIs with higher 5mC levels than GSCs (Figure S5D). Accordingly, while GSCLCs, GSCs, and KIT (−) spermatogonia at P7 exhibited excellent correlation with regard to the 5mC levels of all promoters, GSCLCs showed divergence from GSCs and KIT (−) spermatogonia at P7 with regard to the 5mC levels of differentially methylated promoters, with GSCLC1 (with better spermatogenic activity) and 4 (with no spermatogenic activity) showing better and worse correlations, respectively (Figure 5B).

We identified the promoters and non-promoter CGIs having differential 5mC levels (≧ 25%) between each GSCLC line and the averages of GSCs, which revealed that differential methylation was mainly attributable to hyper-methylation in GSCLCs and exhibited a modest overlap among the GSCLC lines (Figures 5C and S5D; Table S2). The hyper-methylated promoters in GSCLCs constituted ~3.0%–5.4% of all promoters (Figure 5C; Table S2) and enriched with genes for "signal transduction" and "immune system process," whereas the hypo-methylated promoters in GSCLCs were very minor (~0.2%–~0.5%) and were enriched with those for "sensory perception of smell" (Figure S6A; Tables S2 and S3). Importantly, genes bearing hyper-methylated promoters, but not non-promoter CGIs, in GSCLCs (GSCLC − GSC ≧ 25%) exhibited a significant tendency to be

repressed in GSCLCs (Figures 5D and S6B), and such genes included Pou5f1 and genes critical for meiosis/transposon repression through DNA methylation (Sohlh1, Dpep3, Tex19.1, Tdrd9) (Ballow et al., 2006; Ollinger et al., 2008; Shoji et al., 2009; Yoshitake et al., 2011) (Figures 5E and S6C). Genes such as Spo11 (essential for meiosis [Baudat et al., 2000; Romanienko and Camerini-Otero, 2000]) and Piwil1 (essential for spermiogenesis [Deng and Lin, 2002]), which showed no/low expression in GSCs and GSCLCs, also exhibited higher promoter methylation in GSCLCs (Figures 5E and S6C).

We examined the methylation states of the differentially methylated regions (DMRs) of imprinted genes. While the DMRs of paternally imprinted genes (H19, Rasgrf1, and Dlk1-Gtl2) were properly methylated in all GSCLCs, some of the DMRs of maternally imprinted genes exhibited aberrant methylation profiles: while GSCLC1 and 4 showed apparently normal maternal imprints, GSCLC2 and 3 exhibited aberrant methylation in the DMRs of Snrpn and Impact, and Peg1/Mest, Lit1/Kcnq1ot1, Meg1/Grb10, and Impact, respectively (Figures 5F and S6D; Table S4). We then examined the methylation profiles of the transposons. In contrast to the other regulatory elements, GSCLC2, 4, and to a lesser extent, 1, but not 3, exhibited hypo-methylation in the promoters or long terminal repeats (LTRs) of a number of long interspersed nuclear element 1 s (LINE1s) or endogenous retroviruses (ERVs) 1, 2 (including intracisternal A particles [IAPs]), and 3, respectively (Figures 5G and S6E; Table S4). This may be a consequence of the repression of Tex19.1 and Tdrd9 (Figures 4 and 5E), which are critical for transposon repression through DNA methylation of their regulatory elements (Ollinger et al., 2008; Shoji et al., 2009). Consistently, IAPs were de-repressed in GSCLC2 and 4 with the second lowest and the lowest LTR methylation levels, and two classes of LINE1s were de-repressed in GSCLC2 with the lowest promoter methylation levels (Figure S6E). Collectively, these findings show that GSCLC induction from PGCLCs entails line-dependent mis-regulation, in particular, hyper-methylation, of a fraction of regulatory elements that exhibit partial overlaps among the GSCLC lines and such hyper-methylation leads to the repression of associated genes.

Methylation Dynamics of Regulatory Elements Vulnerable to Mis-regulation

We explored a potential cause of aberrant DNA methylation on key regulatory elements during the derivation of GSCLCs. We identified promoters that exhibited higher 5mC levels in all GSCLCs compared to the averages of GSCs (GSCLCs − GSCs ≧ 25%, p < 0.01, Welch's t test, 263 promoters) and examined their methylation dynamics during male germ cell


Figure 4. Comparison of the Transcriptomes of GSCLCs and GSCs

(A–C) UHC (A) and PCA (B and C) of transcriptomes of the indicated cell types.

(D) (left, top) Pie graphs showing the numbers and percentages of DEGs (down in GSCLCs: blue; up in GSCLCs: orange) between each GSCLC line and the averages of two GSC lines among genes expressed in GSCs/GSCLCs (9,073 genes: log2[RPM+1] >4 in at least one line). (left, bottom) Bar graphs showing the overlap of DEGs between each GSCLC line and the averages of two GSC lines. The color coding is as indicated. (right) The list of genes commonly down (top)/up (bottom)-regulated in all four GSCLCs and their GO enrichments are shown.

(E) Heatmap of the expression of the unions of genes up (left)/down (right)-regulated in GSCLCs and their GO enrichments with composite genes. The color coding is as indicated.

See also Figure S4 and Table S1.
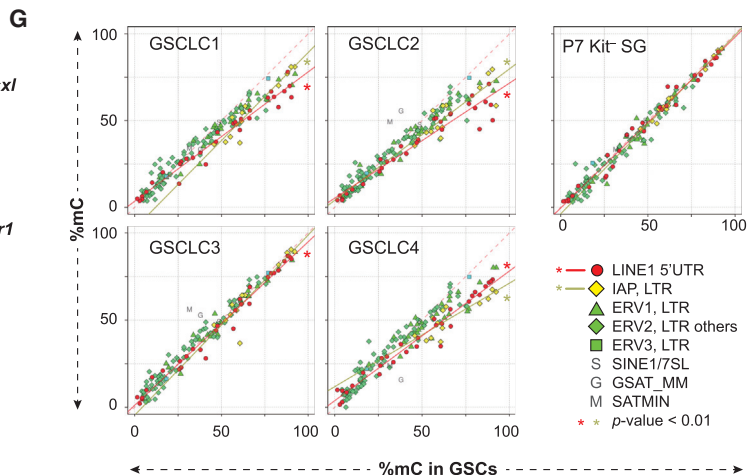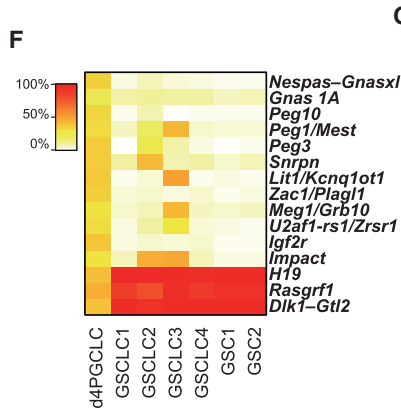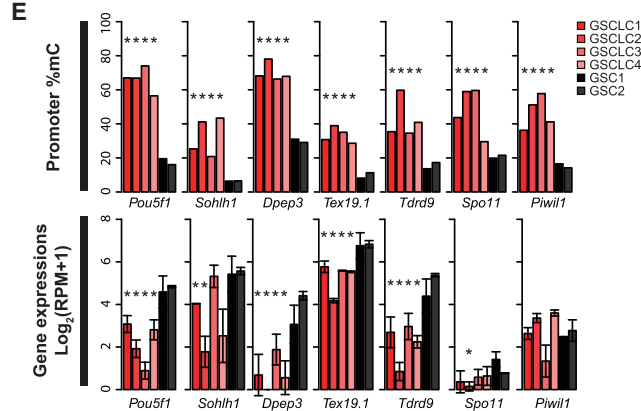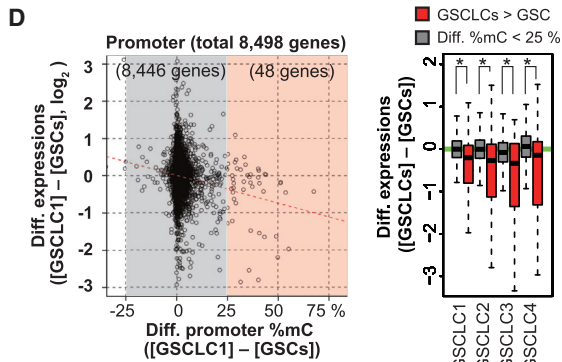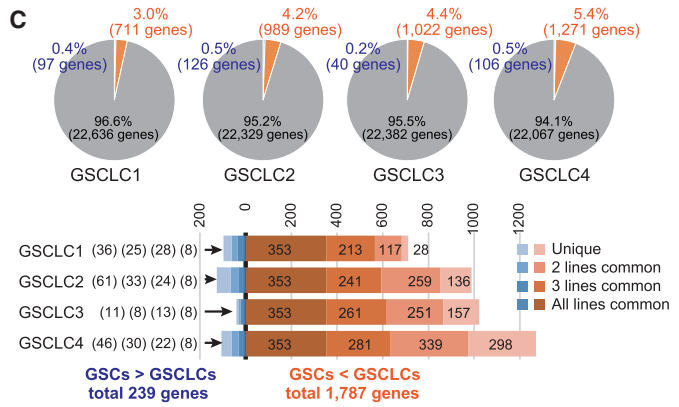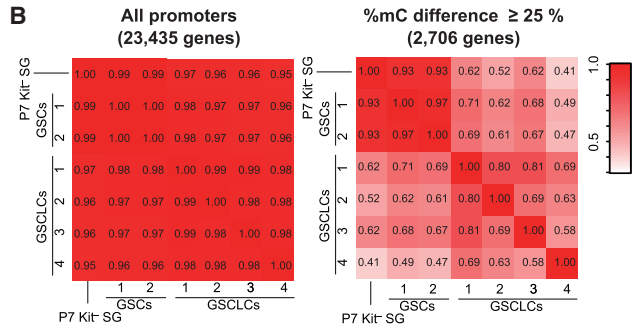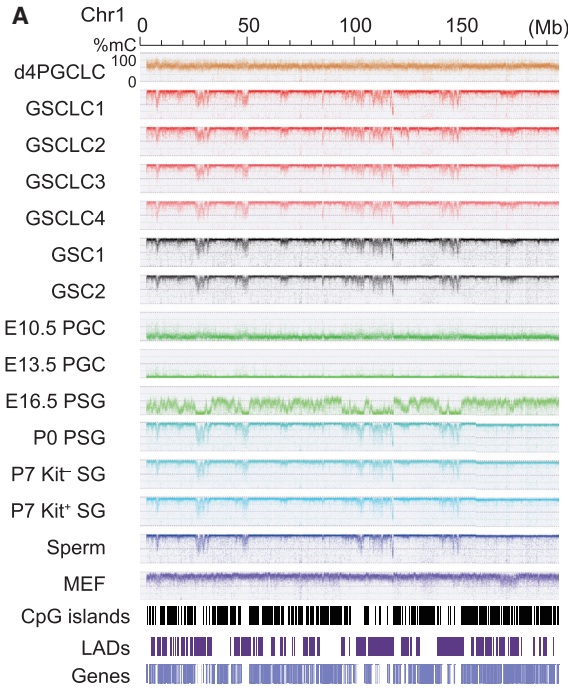
(legend on next page)

development. The differentially methylated promoters exhibit 5mC-level distributions of from 0% to ~75% in d4 PGCLCs and show nearly complete demethylation in male germ cells at E13.5 (Figure 6). During the differentiation of KIT (−) spermatogonia at P7, their 5mC levels, particularly those with higher 5mC levels in d4 PGCLCs, are elevated but remain relatively low (average: ~30.0%), and their 5mC levels in KIT (−) spermatogonia at P7 are similar to those in GSCs (average: ~35.7%) (Figure 6).

In contrast, such promoters exhibited relatively high 5mC levels in GSCLCs (average: GSCLC1: ~73.4%; 2: ~75.9%; 3: ~81.6%; 4: ~81.7%) (Figure 6). We generated a hypothetical 5mC-level plot in which the 5mC levels of these promoters were shown as the simple sum of their levels in d4 PGCLCs and GSCs, which resulted in a 5mC-level distribution pattern (average: ~82.2%) similar to those in GSCLCs (Figure 6). On the other hand, for some of the promoters with relatively low 5mC levels in d4 PGCLCs, GSCLCs exhibited higher 5mC levels than those determined in the hypothetical model (Figure 6). These findings suggest that GSCLCs acquire higher 5mC levels in a fraction of regulatory elements presumably due to a failure in the DNA demethylation (reprogramming) and the suppression of the elevation of DNA methylation levels (programming).

Heterogeneity among GSCLCs and GSCs

We evaluated the potential heterogeneity/clonality of GSCLCs in comparison to that of GSCs by analyzing their single-cell transcriptomes, which are the culmination of their epigenetic states. We generated single-cell cDNAs from GSCLC1 (with better spermatogenic activity) and 4 (with no spermatogenic activity), and from GSC1 and 2, and analyzed those with sufficient quality by single-cell 3-prime RNA sequencing (SC3-seq) (30, 24, 29, and 24 single cells for GSCLC1, 4, GSC1, and 2, respectively) (Figures S7A–S7C) (Nakamura et al., 2015). The DEGs between GSCLCs and GSCs identified by the population-level analyses were represented appropriately in single-cell cDNAs from GSCLCs and GSCs (Figures 7A and S7D). Accordingly, both

UHC and PCA revealed that single cells from GSC1 and 2 generated intermingled clusters, whereas single cells from GSCLC1 and 4 contributed to separate clusters, with single cells from GSCLC1 generating a cluster closer to those of GSCs (Figures 7B and 7C).

To quantify the extent of heterogeneity among single cells, we calculated the variances of the expression levels of individual genes among single cells from GSCLCs and GSCs. This analysis revealed that the distributions of such variances were similar among GSCLCs and GSCs (Figure 7D). Statistical analyses (Kruskal-Wallis test followed by Bonferroni correction) revealed that due to large numbers of genes analyzed, the distribution of gene-expression variances in GSC1 turned out to be different from that in GSC2 ($p = 8.9 \times 10^{-6}$), but, importantly, not different from that in GSCLC1 ($p > 0.1$) (Figure 7D). Furthermore, the gene-expression variance in GSCLC4 was the smallest among those in GSCs and GSCLCs (Figure 7D), indicating that the heterogeneity of GSCLCs is not larger than that of GSCs.

DISCUSSION

We have shown that PGCLCs induced from ESCs can differentiate into spermatogonia-like cells in reconstituted testes and are then propagated as GSCLCs (Figure 7E). GSCLCs differ from PGCLCs in terms of their transcriptome, DNA methylome, and most critically, capacity for undergoing spermatogenesis in adult testes (Figures 3, 4, and 5). Our system therefore represents a stepwise reconstitution of the male germ cell differentiation pathway in vitro, realizing the induction of a stable cell line with SSC function from PSCs (Figure 7E). Compared to GSCs derived from neonatal testes, GSCLCs exhibited a limited capacity for spermatogenesis (Figure 3). GSCLCs bore hyper-methylation in a fraction of promoters and regulatory elements, including at genes critical for meiosis/spermatogenesis and several DMRs of maternally imprinted genes (Figure 5), and such hyper-methylation in promoters is correlated with the repression of associated genes (Figure 5). The observed

---

Figure 5. Comparison of the DNA Methylomes of GSCLCs and GSCs

(A) The 5mC-level tracks across chromosome 1 in the indicated cell types (this study and Kobayashi et al., 2013; Kubo et al., 2015; Shirane et al., 2016). The distributions of CGIs, LADs, and genes are shown at the bottom. PSG, pro-spermatogonia; SG, spermatogonia.

(B) Heatmap of the correlation coefficients among the indicated cells based on the 5mC levels of all promoters (left) or the 5mC levels of differentially methylated promoters (promoters with ≧ 25% 5mC-level differences among GSCLCs/GSCs/ KIT (−) spermatogonia at P7; 2,706 promoters) (right). The color coding is as indicated.

(C) (top) Pie graphs showing the numbers and percentages of differentially methylated promoters (down in GSCLCs: blue; up: orange) between each GSCLC line and the averages of two GSC lines among all promoters (23,444 promoters). (bottom) Bar graphs showing the overlap of differentially methylated promoters. The color coding is as indicated.

(D) (left) Scatterplots for the relationship of gene-expression differences ($\log_2$[RPM+1]) with promoter 5mC-level differences (%5mC levels: gray, <25%; pink, ≧ 25%) between GSCLC1 and the averages of two GSC lines. The numbers of the genes ($\log_2$[RPM+1] >4 in at least one line) are indicated. (right) Boxplots [the averages (horizontal lines), 25th and 75th percentiles (boxes), and fifth and 95th percentiles (error bars)] of gene-expression differences ($\log_2$[RPM+1]) between each GSCLC line and the averages of two GSC lines of genes with promoter 5mC-level differences of <25% (gray) and of ≧ 25% (red). The latter genes exhibited significant repression (*Mann-Whitney-Wilcoxon test, p < 0.01).

(E) Promoter 5mC levels (%5mC) and expression levels ($\log_2$ [RPM+1]) of the indicated genes in the indicated cell types. SDs of the two biological replicates are shown as bars for expression levels. *Statistically significant promoter 5mC-level (Welch's t test [paired], p < 0.01) or expression-level differences (Welch's t test [one sided], p < 0.05) between GSCLCs and GSCs.

(F) Heatmap of the 5mC levels in the gametic DMRs of maternally or paternally imprinted genes in the indicated cell types. The color coding is as indicated.

(G) Scatterplot comparisons of the 5mC levels in the indicated loci between GSCLCs and GSCs. The color coding is as indicated. *Statistically significant LINE1 5′ UTR or IAP LTR 5mC-level differences (5′ UTR or LTR with ≧ 50% of 5mC levels, Welch's t test [paired], p < 0.01) between GSCLCs and GSCs. GSAT_MM, major satellites; SATMIN, minor satellites.
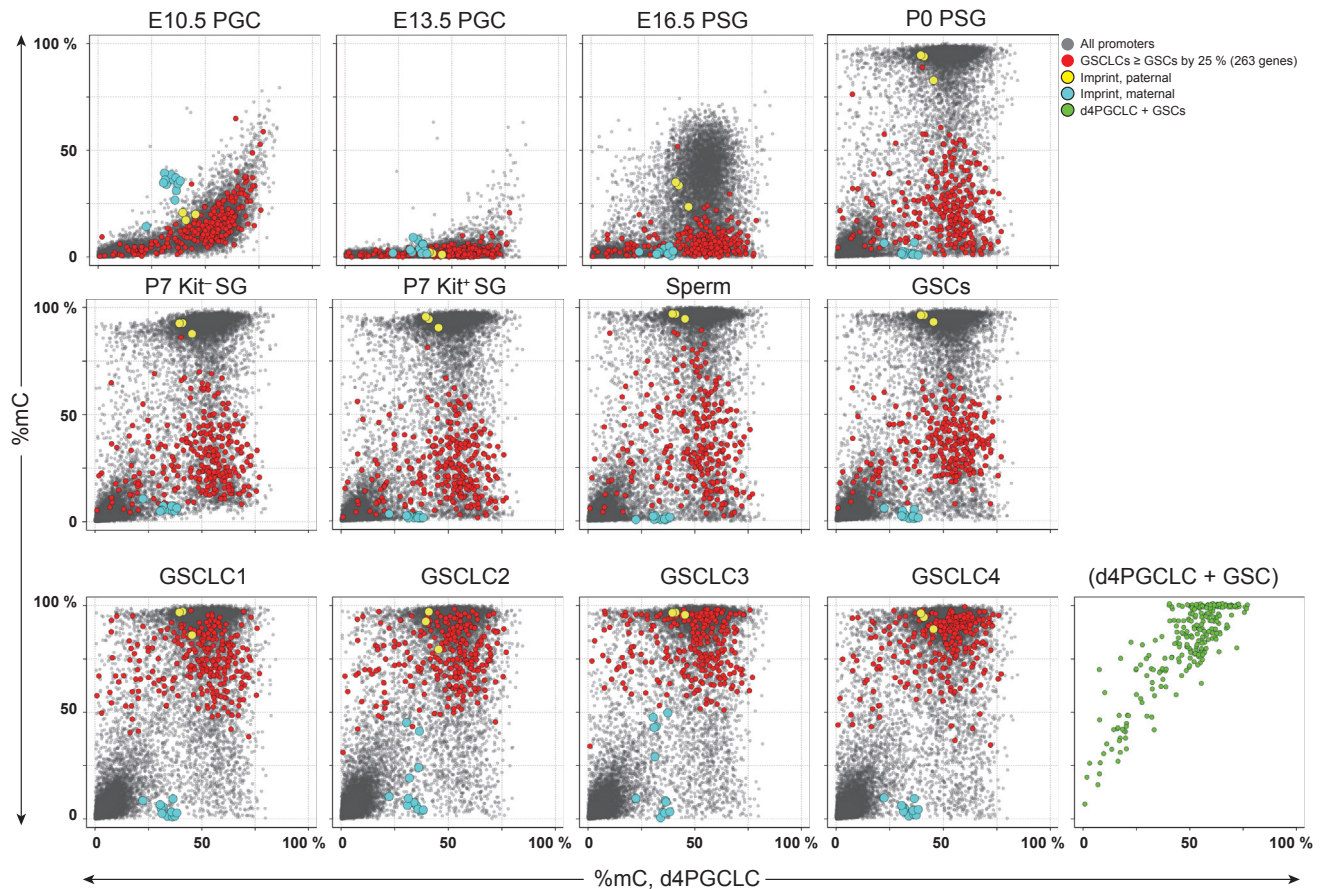
See also Figures S5 and S6 and Tables S2, S3, and S4.

Figure 6. The 5mC-Level Dynamics during Male Germ Cell Development and GSCLC/GSC Derivation

Scatterplot comparisons of promoter 5mC levels between d4PGCLCs and the indicated cell types. Differentially methylated promoters between GSCLCs and GSCs (GSCLCs − GSCs $\geqq$ 25%, Welch's t test [paired]: p < 0.01, 263 promoters) are highlighted by red dots. The simple sum of their levels in d4 PGCLCs and GSCs is shown by green dots (second row, right). The other color coding is as indicated.

See also Figures S5 and S6.

hyper-methylation may be a combinatorial consequence of an incomplete genome-wide DNA demethylation and aberrant DNA methylation during differentiation of PGCLCs into spermatogonia-like cells in reconstituted testes (Figures 6 and 7E), the clarification of which warrants future investigation.

Despite partially aberrant epigenetic properties of GSCLCs (Figures 5 and 6), the offspring from spermatozoa derived from GSCLCs appeared grossly normal and fertile (Figure 3). Since GSCLCs bear a heterogeneity/clonality similar to GSCs (Figure 7), the spermatogenesis and subsequent embryogenesis following fertilization would be a process that tolerates, to some extent, the epigenetic abnormalities, including those in some imprinted genes, of the founding cell population. The mechanism by which epigenotypes that are compatible with normal development and physiology are segregated during spermatogenesis from GSCLCs requires further investigation, including genome-wide DNA methylation analyses of GSCLC-derived spermatocytes, spermatids, and spermatozoa, ideally at single-cell resolution. Alternatively, aberrant epigenotypes might be nullified by epigenetic reprogramming in pre-implantation development (Lee et al., 2014; Saitou et al., 2012). The

possibility that GSCLC-derived offspring bear certain abnormalities through trans-generational epigenetic inheritance (Heard and Martienssen, 2014) will also require rigorous investigation. Indeed, our system should serve as a unique basis for mechanistic studies on trans-generational epigenetic inheritance through the male germline.

In reconstituted ovaries, a majority of PGCLCs interact with ovarian somatic cells and exhibit robust proliferation, epigenetic reprogramming, and entry into meiosis (Hayashi et al., 2012; Hikabe et al., 2016), whereas in reconstituted testes, PGCLCs initially tended to cluster by themselves and only a fraction of them were successfully incorporated into seminiferous tubule-like structures to go on to form spermatogonia-like cells (Figures 1 and S1). Considering that genome-wide DNA demethylation in PGCs appears to be mediated largely through replication-coupled passive demethylation (Kagiwada et al., 2013; Seisenberger et al., 2012; Shirane et al., 2016; Yamaguchi et al., 2012), under the present conditions for reconstituted testes, an initial interaction of PGCLCs with testicular somatic cells for their appropriate proliferation for genome-wide DNA demethylation may not be optimal, and prior to such an event, signals
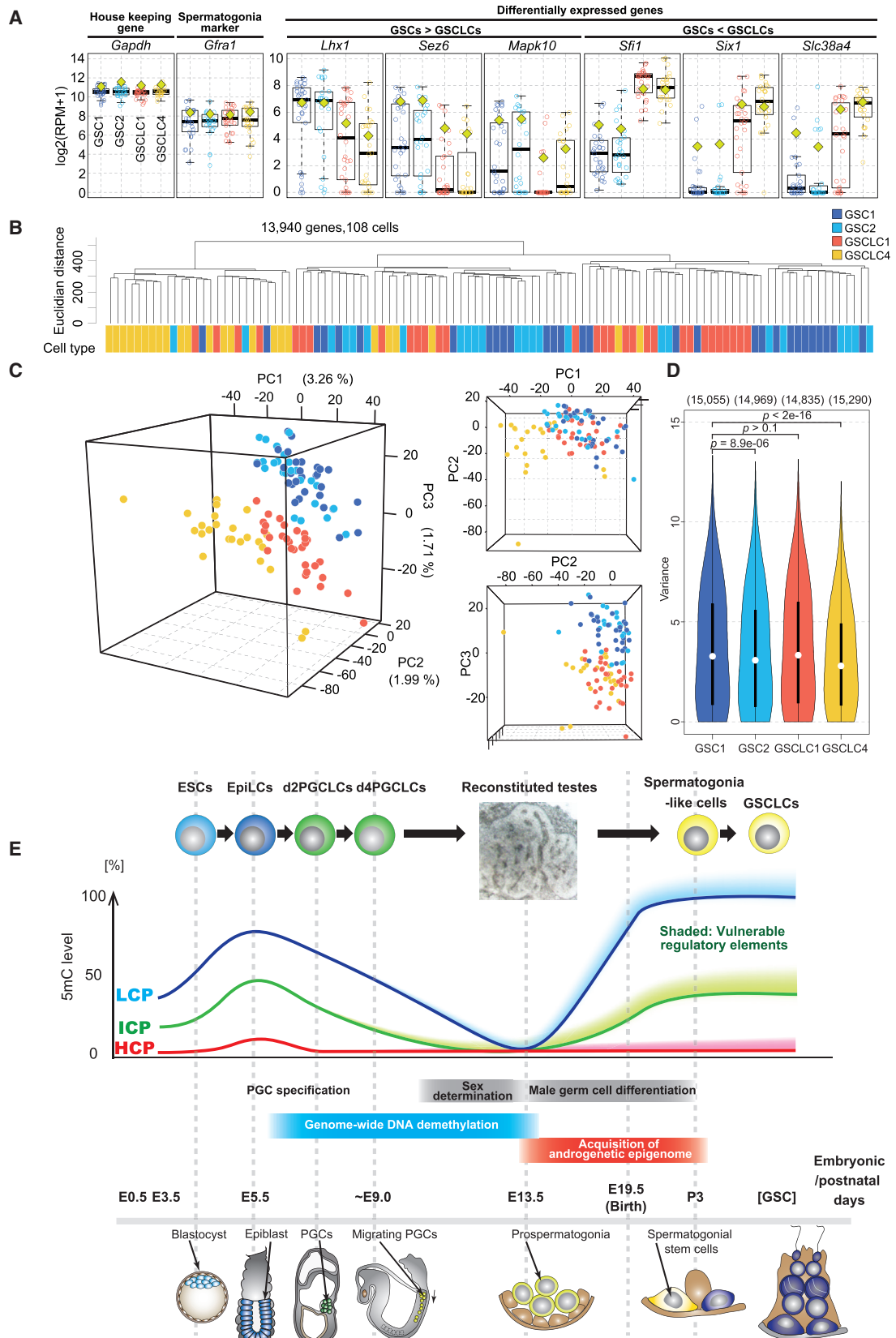
(legend on next page)

reinforcing the androgenetic epigenome may be provided, resulting in the hyper-methylation of a fraction of key regulatory elements. Consistent with this idea, endogenous PGCs at E12.5, which have almost completed genome-wide DNA demethylation (Kobayashi et al., 2013; Seisenberger et al., 2012), underwent differentiation into PLZF (+) spermatogonia-like cells (and most likely into SCP3 (+) spermatocytes) more efficiently than PGCLCs (Figures 1 and S1). Thus, an improvement of culture conditions for reconstituted testes, e.g., by using an appropriate intermediate index for epigenetic reprogramming/proper male germ cell development, or separate culture for PGCLCs for the completion of genome-wide DNA demethylation combined with reconstituted testes, might lead to an induction of spermatogonia-like cells and GSCLCs with better function. Combined with an emerging system for ex vivo maturation of spermatogonia/SSCs into spermatozoa (Komeya et al., 2016; Sato et al., 2011), such improvements would lead to the production of spermatozoa from PSCs entirely in culture.

During the course of this study, it was reported that d6 PGCLCs—when co-cultured with cells dissociated from testes of neonatal W/W^v mice and provided with appropriate cytokines and hormones—entered into and then completed meiosis within 2 weeks and resultant spermatid-like cells contributed to apparently normal offspring (Zhou et al., 2016). Moreover, human fibroblasts were directly induced into haploid cells by overexpression of a combination of transcription factors (PRDM1, PRDM14), translational regulators (LIN28A, DAZL, DDX4) and a component of the synaptonemal complex (SCP3) (Medrano et al., 2016). Our study points to the importance of epigenetic regulation—i.e., genome-wide DNA demethylation followed by appropriate installment of the androgenetic epigenome—for the induction of PGCLCs into spermatogonia-like cells and GSCLCs with proper function. Thus, we consider that the epigenetic landscape of the cells reported in these studies (Medrano et al., 2016; Zhou et al., 2016) will require further investigation (Saitou and Miyauchi, 2016).

EXPERIMENTAL PROCEDURES

All animal experiments were performed under the ethical guidelines of Kyoto University. The experimental procedures for animals, fluorescence-activated Cell Sorting (FACS), magnetic-activated cell sorting (MACS), transplantation of PGCLCs and GSCLCs into testes, intra-cytoplasmic sperm injection (ICSI) and round spermatid injection (ROSI), histology and Immunofluorescence (IF) analysis, alkaline phosphatase (AP) staining, karyotype analysis, qPCR, combined bisulfite restriction analysis (COBRA), RNA-seq analysis, mapping reads of RNA-seq, and conversion to gene expression levels, data analysis of the RNA-seq, whole-genome bisulfite analysis (WGBS), processing, mapping and conversion of the data for bisulfite sequencing, annotation of promoters,

non-promoter CGIs, repetitive elements, and imprint DMRs, analysis of DNA methylation in single-copy genomic loci, promoters, and non-promoter CGIs, analysis of published WGBS data, and antibodies/primers/oligonucleotides used in this study are available in Supplemental Experimental Procedures.

Culture of ESCs and Induction of PGCLCs

ESCs bearing the AAG transgenes (C57BL/6 × 129/SvJcl) (Ohta et al., 2000) were cultured in N2B27 medium with 2i (PD0325901: 0.4 μM [Stemgent]; CHIR99021: 3 μM [Stemgent]) and LIF (1,000 U/mL) on wells coated with poly-L-ornithine and laminin (20 ng/mL) (Hayashi et al., 2011; Hayashi and Saitou, 2013; Ying et al., 2008). Epiblast-like cells (EpiLCs) were induced from 1.0×10^5 ESCs on the wells of a 12-well plate coated with human plasma fibronectin (16.7 g/mL) in EpiLC medium (N2B27 containing activin A [20 ng/mL], bFGF [12 ng/mL], and knockout serum replacement [KSR] [1%] [Thermo Fisher Scientific]). The EpiLC medium was changed every day. PGCLCs were induced from 2.0×10^3 EpiLCs under a floating condition in a low-cell-binding U-bottom 96-well Lipidure-Coat Plate in PGCLC medium (GMEM [Invitrogen] with 15% KSR, 0.1 mM NEAA, 1 mM sodium pyruvate, 0.1 mM 2-mercaptoethanol, 100 U/mL penicillin, 0.1 mg/mL streptomycin, and 2 mM L-glutamine with BMP4 [500 ng/mL] [R&D Systems], LIF [1,000 U/mL] [Invitrogen], SCF [100 ng/mL] [R&D Systems], and EGF [50 ng/mL] [R&D Systems] for 4–6 days).

Generation and Culture of Reconstituted Testes

The d4 PGCLCs collected by FACS (10,000 cells/reconstituted testis) (see fluorescence-activated cell sorting) were aggregated with somatic cells of E12.5 gonads (ICR) collected by MACS (40,000 cells/ reconstituted testis) (see magnetic-activated cell sorting) under a floating condition in a low-cell-binding U-bottom 96-well Lipidure-Coat Plate in α-Minimum Essential Medium (α-MEM) (Invitrogen) containing 10% KSR (37°C, 5% CO$_2$). After floating culture for 2 days, the aggregates were transferred to wells of a Falcon Permeable Support for 24-Well Plates with a 0.4 μm transparent PET membrane (Corning) using a glass capillary. Each well was supplemented with 350 μL of αMEM-10%KSR for a gas-liquid interphase culture (Sato et al., 2011). The medium was changed every week.

Derivation of GSCLCs from Reconstituted Testes and of GSCs from Neonatal Testes

Reconstituted testes were soaked in the dissociation buffer (DMEM containing dispase [1 mg/mL] [Invitrogen] and hyaluronidase [1 mg/mL] [Sigma, H3506]) for 10 min and then incubated with 0.05% Trypsin-0.53 mM EDTA for 15 min with periodic pipetting (every 5 min), which was quenched in DMEM with 10% FBS, followed by dissociation into single cells by rigorous pipetting. The cell suspension was centrifuged at 1,200 rpm for 5 min and the supernatant was removed. The cell pellet was suspended in the GSC/GSCLC culture medium with growth factors (see below), and the cells were plated on a 0.1% (w/v) gelatin-coated culture plate (the cells/reconstituted testis were transferred to one 24-well plate). The somatic cells were removed as much as possible by repeated passages every 12 hr, as somatic cells bind more easily to the culture plate. After two or three passages, the remaining AAG (+) cells were transferred onto plates with MEFs in GSC/GSCLC medium with growth factors (see below). We noted that, when more than approximately 1×10^3 AAG (+) cells/well were plated, GSCLC colonies were expanded during the first 2 weeks. When GSCLC colonies of more than approximately 500 μm in diameter developed, they were passaged into a new well and the GSCLC lines were established after approximately 2 months. The control GSC lines were derived

Figure 7. Single-Cell Transcriptome Analyses of GSCLCs and GSCs

(A) Expression levels of the indicated genes in the indicated cell types analyzed at the single-cell (boxplots) or population (green squares) levels. 30 (GSCLC1), 24 (GSCLC4), 29 (GSC1), and 24 (GSC2) single cells were analyzed. In boxplots, the median (horizontal lines), 25th and 75th percentiles (boxes), and the outlier points (>2 SDs, error bars), and the values for each cell are indicated.

(B and C) UHC (B) and PCA (C) of single-cell transcriptomes of GSCLCs and GSCs. The color coding is as indicated.

(D) The distributions of the variances of the expression levels of individual genes (numbers indicated) among indicated single cells. The differences of the variance distributions compared to those of GSC1 are analyzed by Kruskal-Wallis test followed by Bonferroni correction and the p values are shown.

(E) A model for the relationship between male germ cell development in vivo and in vitro, with reference to DNA methylation reprogramming/programming in promoters.

See also Figure S7 and Table S5.

from neonatal testes at P7 (129/Sv × C57BL/6 with AAG) by using essentially the same procedure.

The medium for GSCs/GSCLCs culture was as described in Kanatsu-Shinohara et al. (2003) with some modifications: StemPro-34 SFM (Invitrogen) was supplemented with StemPro supplement (Invitrogen), 1% FBS, 1 × GlutaMAX-I(Invitrogen), 1 × minimal essential medium (MEM) Vitamin Solution (Sigma), 5 mg/mL AlbuMAX-II (Invitrogen), 5×10^{-5} M 2-mercaptoethanol, 1 × MEM nonessential amino acid solution (Invitrogen), 30 μg/mL pyruvic acid, 1 × ITS-G (Invitrogen), 100 U/mL penicillin, 0.1 mg/mL streptomycin, and growth factors (recombinant rat GDNF [10 ng/mL] [R&D Systems], human bFGF [10 ng/mL] [Invitrogen], LIF/ESGRO [10^3 U/mL] [Invitrogen], and mouse EGF [20 ng] [Invitrogen]).

ACCESSION NUMBERS

The accession numbers for the RNA-seq data of GSC1, 2 and GSCLC1–4, the SC3-seq data of GSC1, 2, GSCLC1 and 4, the WGBS data of GSC1 and GSCLC1-3, and the WGBS data of GSC2 and GSCLC4 reported in this paper are NCBI GEO: GSE76245, GSE87341, DDBJ: DRA004241, and DRA005141, respectively.

SUPPLEMENTAL INFORMATION

Supplemental Information includes Supplemental Experimental Procedures, seven figures, and five tables and can be found with this article online at http://dx.doi.org/10.1016/j.celrep.2016.11.026.

AUTHOR CONTRIBUTIONS

ACKNOWLEDGMENTS

REFERENCES

Ballow, D., Meistrich, M.L., Matzuk, M., and Rajkovic, A. (2006). Sohlh1 is essential for spermatogonial differentiation. Dev. Biol. *294*, 161–167.

Baudat, F., Manova, K., Yuen, J.P., Jasin, M., and Keeney, S. (2000). Chromosome synapsis defects and sexually dimorphic meiotic progression in mice lacking Spo11. Mol. Cell *6*, 989–998.

Bellvé, A.R., Cavicchia, J.C., Millette, C.F., O'Brien, D.A., Bhatnagar, Y.M., and Dym, M. (1977). Spermatogenic cells of the prepuberal mouse. Isolation and morphological characterization. J. Cell Biol. *74*, 68–85.

Brinster, R.L., and Zimmermann, J.W. (1994). Spermatogenesis following male germ-cell transplantation. Proc. Natl. Acad. Sci. USA *91*, 11298–11302.

Buaas, F.W., Kirsh, A.L., Sharma, M., McLean, D.J., Morris, J.L., Griswold, M.D., de Rooij, D.G., and Braun, R.E. (2004). Plzf is required in adult male germ cells for stem cell self-renewal. Nat. Genet. *36*, 647–652.

Chuma, S., Kanatsu-Shinohara, M., Inoue, K., Ogonuki, N., Miki, H., Toyokuni, S., Hosokawa, M., Nakatsuji, N., Ogura, A., and Shinohara, T. (2005). Spermatogenesis from epiblast and primordial germ cells following transplantation into postnatal mouse testis. Development *132*, 117–122.

Costoya, J.A., Hobbs, R.M., Barna, M., Cattoretti, G., Manova, K., Sukhwani, M., Orwig, K.E., Wolgemuth, D.J., and Pandolfi, P.P. (2004). Essential role of Plzf in maintenance of spermatogonial stem cells. Nat. Genet. *36*, 653–659.

Deng, W., and Lin, H. (2002). miwi, a murine homolog of piwi, encodes a cytoplasmic protein essential for spermatogenesis. Dev. Cell *2*, 819–830.

Fujiwara, Y., Komiya, T., Kawabata, H., Sato, M., Fujimoto, H., Furusawa, M., and Noce, T. (1994). Isolation of a DEAD-family protein gene that encodes a murine homolog of Drosophila vasa and its specific expression in germ cell lineage. Proc. Natl. Acad. Sci. USA *91*, 12258–12262.

Ginsburg, M., Snow, M.H., and McLaren, A. (1990). Primordial germ cells in the mouse embryo during gastrulation. Development *110*, 521–528.

Guelen, L., Pagie, L., Brasset, E., Meuleman, W., Faza, M.B., Talhout, W., Eussen, B.H., de Klein, A., Wessels, L., de Laat, W., and van Steensel, B. (2008). Domain organization of human chromosomes revealed by mapping of nuclear lamina interactions. Nature *453*, 948–951.

Hayashi, K., and Saitou, M. (2013). Generation of eggs from mouse embryonic stem cells and induced pluripotent stem cells. Nat. Protoc. *8*, 1513–1524.

Hayashi, K., Ohta, H., Kurimoto, K., Aramaki, S., and Saitou, M. (2011). Reconstitution of the mouse germ cell specification pathway in culture by pluripotent stem cells. Cell *146*, 519–532.

Hayashi, K., Ogushi, S., Kurimoto, K., Shimamoto, S., Ohta, H., and Saitou, M. (2012). Offspring from oocytes derived from in vitro primordial germ cell-like cells in mice. Science *338*, 971–975.

Hayatsu, H., and Shiragami, M. (1979). Reaction of bisulfite with the 5-hydroxymethyl group in pyrimidines and in phage DNAs. Biochemistry *18*, 632–637.

Heard, E., and Martienssen, R.A. (2014). Transgenerational epigenetic inheritance: Myths and mechanisms. Cell *157*, 95–109.

Hikabe, O., Hamazaki, N., Nagamatsu, G., Obata, Y., Hirao, Y., Hamada, N., Shimamoto, S., Imamura, T., Nakashima, K., Saitou, M., and Hayashi, K. (2016). Reconstitution in vitro of the entire cycle of the mouse female germ line. Nature *539*, 299–303.

Hilscher, B., Hilscher, W., Bülthoff-Ohnolz, B., Krämer, U., Birke, A., Pelzer, H., and Gauss, G. (1974). Kinetics of gametogenesis. I. Comparative histological and autoradiographic studies of oocytes and transitional prospermatogonia during oogenesis and prespermatogenesis. Cell Tissue Res. *154*, 443–470.

Illingworth, R.S., Gruenewald-Schneider, U., Webb, S., Kerr, A.R., James, K.D., Turner, D.J., Smith, C., Harrison, D.J., Andrews, R., and Bird, A.P. (2010). Orphan CpG islands identify numerous conserved promoters in the mammalian genome. PLoS Genet. *6*, e1001134.

Irie, N., Weinberger, L., Tang, W.W., Kobayashi, T., Viukov, S., Manor, Y.S., Dietmann, S., Hanna, J.H., and Surani, M.A. (2015). SOX17 is a critical specifier of human primordial germ cell fate. Cell *160*, 253–268.

Kagiwada, S., Kurimoto, K., Hirota, T., Yamaji, M., and Saitou, M. (2013). Replication-coupled passive DNA demethylation for the erasure of genome imprints in mice. EMBO J. *32*, 340–353.

Kanatsu-Shinohara, M., and Shinohara, T. (2013). Spermatogonial stem cell self-renewal and development. Annu. Rev. Cell Dev. Biol. *29*, 163–187.

Kanatsu-Shinohara, M., Ogonuki, N., Inoue, K., Miki, H., Ogura, A., Toyokuni, S., and Shinohara, T. (2003). Long-term proliferation in culture and germline transmission of mouse male germline stem cells. Biol. Reprod. *69*, 612–616.

Kobayashi, H., Sakurai, T., Miura, F., Imai, M., Mochiduki, K., Yanagisawa, E., Sakashita, A., Wakai, T., Suzuki, Y., Ito, T., et al. (2013). High-resolution DNA methylome analysis of primordial germ cells identifies gender-specific reprogramming in mice. Genome Res. *23*, 616–627.

Komeya, M., Kimura, H., Nakamura, H., Yokonishi, T., Sato, T., Kojima, K., Hayashi, K., Katagiri, K., Yamanaka, H., Sanjo, H., et al. (2016). Long-term ex vivo maintenance of testis tissues producing fertile sperm in a microfluidic device. Sci. Rep. *6*, 21472.

Kubo, N., Toh, H., Shirane, K., Shirakawa, T., Kobayashi, H., Sato, T., Sone, H., Sato, Y., Tomizawa, S., Tsurusaki, Y., et al. (2015). DNA methylation and gene expression dynamics during spermatogonial stem cell differentiation in the early postnatal mouse testis. BMC Genomics 16, 624.

Kubota, H., Avarbock, M.R., and Brinster, R.L. (2004). Growth factors essential for self-renewal and expansion of mouse spermatogonial stem cells. Proc. Natl. Acad. Sci. USA 101, 16489–16494.

Lawson, K.A., Dunn, N.R., Roelen, B.A., Zeinstra, L.M., Davis, A.M., Wright, C.V., Korving, J.P., and Hogan, B.L. (1999). Bmp4 is required for the generation of primordial germ cells in the mouse embryo. Genes Dev. 13, 424–436.

Lee, H.J., Hore, T.A., and Reik, W. (2014). Reprogramming the methylome: Erasing memory and creating diversity. Cell Stem Cell 14, 710–719.

Matsui, Y., Zsebo, K., and Hogan, B.L. (1992). Derivation of pluripotential embryonic stem cells from murine primordial germ cells in culture. Cell 70, 841–847.

McGee, E.A., and Hsueh, A.J. (2000). Initial and cyclic recruitment of ovarian follicles. Endocr. Rev. 21, 200–214.

Medrano, J.V., Martínez-Arroyo, A.M., Míguez, J.M., Moreno, I., Martínez, S., Quiñonero, A., Díaz-Gimeno, P., Marqués-Marí, A.I., Pellicer, A., Remohí, J., and Simón, C. (2016). Human somatic cells subjected to genetic induction with six germ line-related factors display meiotic germ cell-like features. Sci. Rep. 6, 24956.

Nakamura, T., Yabuta, Y., Okamoto, I., Aramaki, S., Yokobayashi, S., Kurimoto, K., Sekiguchi, K., Nakagawa, M., Yamamoto, T., and Saitou, M. (2015). SC3-seq: A method for highly parallel and quantitative measurement of single-cell gene expression. Nucleic Acids Res. 43, e60.

Oatley, J.M., Avarbock, M.R., Telaranta, A.I., Fearon, D.T., and Brinster, R.L. (2006). Identifying genes important for spermatogonial stem cell self-renewal and survival. Proc. Natl. Acad. Sci. USA 103, 9524–9529.

Ohbo, K., Yoshida, S., Ohmura, M., Ohneda, O., Ogawa, T., Tsuchiya, H., Kuwana, T., Kehler, J., Abe, K., Schöler, H.R., and Suda, T. (2003). Identification and characterization of stem cells in prepubertal spermatogenesis in mice. Dev. Biol. 258, 209–225.

Ohinata, Y., Ohta, H., Shigeta, M., Yamanaka, K., Wakayama, T., and Saitou, M. (2009). A signaling principle for the specification of the germ cell lineage in mice. Cell 137, 571–584.

Ohta, H., Yomogida, K., Yamada, S., Okabe, M., and Nishimune, Y. (2000). Real-time observation of transplanted 'green germ cells': Proliferation and differentiation of stem cells. Dev. Growth Differ. 42, 105–112.

Ohta, H., Wakayama, T., and Nishimune, Y. (2004). Commitment of fetal male germ cells to spermatogonial stem cells during mouse embryonic development. Biol. Reprod. 70, 1286–1291.

Ollinger, R., Childs, A.J., Burgess, H.M., Speed, R.M., Lundegaard, P.R., Reynolds, N., Gray, N.K., Cooke, H.J., and Adams, I.R. (2008). Deletion of the pluripotency-associated Tex19.1 gene causes activation of endogenous retroviruses and defective spermatogenesis in mice. PLoS Genet. 4, e1000199.

Resnick, J.L., Bixler, L.S., Cheng, L., and Donovan, P.J. (1992). Long-term proliferation of mouse primordial germ cells in culture. Nature 359, 550–551.

Romanienko, P.J., and Camerini-Otero, R.D. (2000). The mouse Spo11 gene is required for meiotic chromosome synapsis. Mol. Cell 6, 975–987.

Saitou, M., and Miyauchi, H. (2016). Gametogenesis from pluripotent stem cells. Cell Stem Cell 18, 721–735.

Saitou, M., Barton, S.C., and Surani, M.A. (2002). A molecular programme for the specification of germ cell fate in mice. Nature 418, 293–300.

Saitou, M., Kagiwada, S., and Kurimoto, K. (2012). Epigenetic reprogramming in mouse pre-implantation development and primordial germ cells. Development 139, 15–31.

Sasaki, K., Yokobayashi, S., Nakamura, T., Okamoto, I., Yabuta, Y., Kurimoto, K., Ohta, H., Moritoki, Y., Iwatani, C., Tsuchiya, H., et al. (2015). Robust In Vitro Induction of Human Germ Cell Fate from Pluripotent Stem Cells. Cell Stem Cell 17, 178–194.

Sato, T., Katagiri, K., Gohbara, A., Inoue, K., Ogonuki, N., Ogura, A., Kubota, Y., and Ogawa, T. (2011). In vitro production of functional sperm in cultured neonatal mouse testes. Nature 471, 504–507.

Seisenberger, S., Andrews, S., Krueger, F., Arand, J., Walter, J., Santos, F., Popp, C., Thienpont, B., Dean, W., and Reik, W. (2012). The dynamics of genome-wide DNA methylation reprogramming in mouse primordial germ cells. Mol. Cell 48, 849–862.

Shirane, K., Kurimoto, K., Yabuta, Y., Yamaji, M., Satoh, J., Ito, S., Watanabe, A., Hayashi, K., Saitou, M., and Sasaki, H. (2016). Global Landscape and Regulatory Principles of DNA Methylation Reprogramming for Germ Cell Specification by Mouse Pluripotent Stem Cells. Dev. Cell 39, 87–103.

Shoji, M., Tanaka, T., Hosokawa, M., Reuter, M., Stark, A., Kato, Y., Kondoh, G., Okawa, K., Chujo, T., Suzuki, T., et al. (2009). The TDRD9-MIWI2 complex is essential for piRNA-mediated retrotransposon silencing in the mouse male germline. Dev. Cell 17, 775–787.

Stadler, M.B., Murr, R., Burger, L., Ivanek, R., Lienert, F., Schöler, A., van Nimwegen, E., Wirbelauer, C., Oakeley, E.J., Gaidatzis, D., et al. (2011). DNA-binding factors shape the mouse methylome at distal regulatory regions. Nature 480, 490–495.

Steinberger, A., Steinberger, E., and Perloff, W.H. (1964). Mammalian testes in organ culture. Exp. Cell Res. 36, 19–27.

Svingen, T., and Koopman, P. (2013). Building the mammalian testis: Origins, differentiation, and assembly of the component cell populations. Genes Dev. 27, 2409–2426.

Tam, P.P., and Snow, M.H. (1981). Proliferation and migration of primordial germ cells during compensatory growth in mouse embryos. J. Embryol. Exp. Morphol. 64, 133–147.

Vidal, V.P., Chaboissier, M.C., de Rooij, D.G., and Schedl, A. (2001). Sox9 induces testis development in XX transgenic mice. Nat. Genet. 28, 216–217.

Viger, R.S., Mertineit, C., Trasler, J.M., and Nemer, M. (1998). Transcription factor GATA-4 is expressed in a sexually dimorphic pattern during mouse gonadal development and is a potent activator of the Müllerian inhibiting substance promoter. Development 125, 2665–2675.

Weber, M., Hellmann, I., Stadler, M.B., Ramos, L., Pääbo, S., Rebhan, M., and Schübeler, D. (2007). Distribution, silencing potential and evolutionary impact of promoter DNA methylation in the human genome. Nat. Genet. 39, 457–466.

Wu, X., Goodyear, S.M., Tobias, J.W., Avarbock, M.R., and Brinster, R.L. (2011). Spermatogonial stem cell self-renewal requires ETV5-mediated downstream activation of Brachyury in mice. Biol. Reprod. 85, 1114–1123.

Yamaguchi, S., Hong, K., Liu, R., Shen, L., Inoue, A., Diep, D., Zhang, K., and Zhang, Y. (2012). Tet1 controls meiosis by regulating meiotic gene expression. Nature 492, 443–447.

Yang, Q.E., and Oatley, J.M. (2014). Spermatogonial stem cell functions in physiological and pathological conditions. Curr. Top. Dev. Biol. 107, 235–267.

Ying, Q.L., Wray, J., Nichols, J., Batlle-Morera, L., Doble, B., Woodgett, J., Cohen, P., and Smith, A. (2008). The ground state of embryonic stem cell self-renewal. Nature 453, 519–523.

Yoshitake, H., Yanagida, M., Maruyama, M., Takamori, K., Hasegawa, A., and Araki, Y. (2011). Molecular characterization and expression of dipeptidase 3, a testis-specific membrane-bound dipeptidase: Complex formation with TEX101, a germ-cell-specific antigen in the mouse testis. J. Reprod. Immunol. 90, 202–213.

Yuan, L., Liu, J.G., Zhao, J., Brundell, E., Daneholt, B., and Höög, C. (2000). The murine SCP3 gene is required for synaptonemal complex assembly, chromosome synapsis, and male fertility. Mol. Cell 5, 73–83.

Zhou, Q., Wang, M., Yuan, Y., Wang, X., Fu, R., Wan, H., Xie, M., Liu, M., Guo, X., Zheng, Y., et al. (2016). Complete meiosis from embryonic stem cell-derived germ cells in vitro. Cell Stem Cell 18, 330–340.